Additively Manufactured Hemp Fibers Reinforced Silicone

Pantea Koushki

A Thesis
In
The Department
Of
Mechanical, Industrial and Aerospace Engineering (MIAE)

Presented in Partial Fulfillment of the Requirements
for the Degree of Master of Applied Science
Concordia University
Montréal, Québec, Canada

Winter 2019

Concordia University
School of Graduate Studies

This is to certify that the thesis prepared

By: **Pantea Koushki**

Entitled: **Additively Manufactured Hemp Fibers Reinforced Silicone**

and submitted in partial fulfillment of the requirements for the degree of

Master of Applied Science

complies with the regulations of this University and meets the accepted standards with respect to originality and quality.

Signed by the final examining commitee:

Dr. Susan Liscouet-Hanke _____ Chair

Dr. Lucas Hof _____ External Examiner

Dr. Lyas Kadem _____ Examiner

Dr. Tsz Ho Kwok _____ Supervisor

Dr. Rolf Wuthrich _____ Supervisor

Approved _____
Chair of Department or Graduate Program Director

_____ 20 _____ _____
Dean

Abstract

Additively Manufactured Hemp Fibers Reinforced Silicone

Pantea Koushki

Additive manufacturing provides a broad range of applications and offers significant advantages over conventional molding methods. One of the advantages with additive manufacturing is its high efficiency of feedstock utilization. Although, the most common polymer and metallic composites feedstocks used within additive manufacturing are normally obtained from inefficient, and non-sustainable sources. This contribution explores the 3D printability of a new material based on silicone and hemp fibers from renewable, sustainable and non-petroleum resources with the aim of enhancing mechanical properties of silicone.

To improve composites printing technology, it's required to discover the desired mixing composition. At first, to determine the proper amount of fibers, samples were fabricated by molding. Incorporation of fibers improved the mechanical properties of the silicone matrix. However, fibers distribution within the matrix adversely affected the printability of silicone due to the resulting high viscosity. Therefore, behavior of the new manufactured material with varying fiber and solvent composition was analyzed using rheological study to obtain a printable material. The composition containing 15 (wt%) hemp fibers and 20 (wt%) solvent with enhanced mechanical properties displayed desirable printability. Moreover, the mechanical properties of the 3D printed and molded samples were studied. The results revealed that 3D printed samples outperformed the molded counterparts in tensile strength and hardness. Finally, a simple gripper and honeycomb structure were fabricated to demonstrate the application of the developed material.

Acknowledgments

This thesis would not have been possible unless with wonderful support and help of my supervisors, Dr. Tsz Ho Kwok, and Dr. Rolf Wüthrich, who encouraged me throughout the entire MASc thesis program; I owe my deepest gratitude to them. It has been my great honor and privilege to work under their supervision.

I am also grateful to Dr. Lucas Hof who assisted me a lot with my research and his generous and knowledgeable suggestions.

I would like to thank my colleagues, Eder Sales, and Yasuo Ignacio Maidana Preze who helped me with their experience and knowledge.

And last but not least, I am indebted to my parents and my sister for their lovely supports and inspiration throughout my life which led me to where I am right now, and my dear boyfriend Roham for his unconditional love and support. With all my love, I dedicate this thesis to you. This accomplishment would not have been possible without them.

Contents

List of Figures **viii**

List of Tables **x**

1 Introduction **1**

1.1 Research plan 4

1.2 Thesis outline 5

2 Literature review **6**

2.1 Composites 7

2.2 Composites of elastomers and natural fibers 8

2.2.1 Natural fibers 8

2.2.2 Elastomeric Composites 9

2.2.3 Natural Fiber Treatment and Characterization 10

2.3 Fabrication technique 13

2.3.1 Additive manufacturing 14

2.3.2 3D printing of polymer matrix composites 14

2.3.3 3D printing silicone 18

3 Experimental procedure **21**

3.1 Introduction 22

3.2 Material 22

3.3 Fiber surface modification 22

3.3.1 Alkali treatment 23

3.3.2 Silane treatment 23

3.4 Fabricating composite based on silicone/hemp 24

3.4.1 Molding 25
3.5 Silicone/hemp fiber composites characterization 26
3.5.1 Mechanical Characterization 26
3.5.2 Fourier transform infrared spectrometry (FT-IR) 27
3.5.3 Scanning electron microscopy 27
3.6 3D printing 27
3.6.1 Printability assessment method 28
3.6.2 3D printing parameters 29
3.6.3 Step 1: Rheological evaluations 31
3.6.4 Step 2: Physical validation 34
3.7 Gripper fabrication and testing 35
3.7.1 Grip Force Measurement 35

4 Results and discussion **38**
4.1 Introduction 39
4.2 Effect of fiber loading and chemical treatment on mechanical properties 40
4.2.1 Tensile Strength and Modulus of molded Composites 40
4.2.2 Hardness of molded Composites 42
4.2.3 Interfacial interaction between fiber/matrix (FTIR) 44
4.2.4 Morphology of the hemp fibers (SEM) 45
4.2.5 Effect of chemical treatment on interaction between fiber and matrix 46
4.3 Printability assessment 48
4.3.1 Rheological evaluation 49
4.3.2 Physical validation 52
4.3.3 Rheological behavior of final printed composites 54
4.4 Effect of 3D printing on mechanical properties of hemp fiber reinforced silicone 55
4.5 Applications 58
4.5.1 Soft robotics 58
4.5.2 Biomedical engineering 60

5 Conclusion and Future works **61**
5.1 Conclusion 62

5.2 Future work 64

List of Figures

1 Sustainable 3D-printing of composites based on plant material. 4
2 Different types of composites. 7
3 Different types of natural fibers. 9
4 Effect of alkali and silane modification on a natural fiber surface . . . 12
5 Include short caption without citations 14
6 Comparison of mechanical properties of printed and non-printed composites 17
7 Four-chambered actuator 19
8 3D-Printed soft robots 20
9 SEM micrographs of hemp fibers. 22
10 Surface modification of hemp fiber using alkali treatment 23
11 Surface modification of hemp fiber silane treatment 24
12 Conditioning vacuum mixer ARV-200 24
13 Molded hemp fiber reinforced silicone composites. 25
14 Tension Test Specimens for silicone 26
15 Ultimaker and the Discov3ry paste extruder. 28
16 Schematic of the proposed research method to determine printability of the designed material. 29
17 Dissolving silicone/Hemp fiber in solvent. 29
18 Shear stress-shear rate results for all experimental samples 32
19 Designed gripper. 35
20 a):Arduino official original UNO R3 microcontroller control board with data line. b): LCD shield module display V3 for Arduino UNO R3. . 35
21 Force measurement device 36
22 A simple voltage divider. 36
23 Voltage as a function of weight. 37

24 Tensile strength of molded hemp fiber reinforced silicone composites. 41
25 Young's modulus of molded hemp fiber reinforced silicone composites. 41
26 Hardness of molded hemp fiber reinforced silicone composites. 42
27 Elongation at break of molded hemp fiber reinforced silicone composites. 43
28 Fourier transform infrared (FTIR) spectrum for treated and untreated hemp fiber. 44
29 SEM images of untreated and treated hemp 46
30 Fractured surface of untreated hemp fiber reinforced silicone. 46
31 Fractured surface of NaOH/silane treated hemp fiber reinforced silicone. 47
32 Effect of fiber incorporation on material flow a)Pure silicone. b)Silicone/hemp fiber. 48
33 Shear-viscosity results for all experimental samples. 49
34 Recovery behavior of experimental samples to determine material behavior under a shear rate ($100s^{-1}$) to near-zero shear to simulate the environment experienced by the materials during extrusion printing. . 50
35 Shear stress ramp for all experimental samples. 51
36 Effect of solvent concentration on material flow; a) 10 (%) solvent b) 20 (%) solvent c) 30 (%) solvent d) 40 (%) solvent. 53
37 Effect of solvent concentration on 3D printing shape fidelity. 53
38 The effect of hemp fibers on shear storage modulus of silicone. 54
39 Mechanical properties of 3D printed products 55
40 Cross-section of 3D printed and molded samples 56
41 Effect of 3D-printing on fiber's orientation. 56
42 Hemp fibers were aligned during extrusion. 57
43 Simple gripper fabricated using DIW 3D printing method 58
44 Using micro force sensor to find the differences between two grippers 59
45 Voltage as a function of weight. 59
46 Fabrication of honeycomb structure with hemp fiber reinforced silicone composite. 60

List of Tables

1 Material properties of natural fibers. 10
2 Mechanical properties of common elastomers 11
3 Different techniques for 3D printing polymers 15
4 Different 3D printing method for fabricating polymer composites reinforced by particles 16
5 Specimen Dimensions in (mm) 26
6 Optimized 3D printing parameters for fabricating silicone 30
7 3D printing parameters for fabricating silicone/hemp fibers. 31
8 K and N coefficients for all experimental samples. 33
9 Shear rate inside nozzle. 34
10 IR absorption of functional groups. 45
11 Yield point of the different samples. 52

Chapter 1

Introduction

Silicone is a polymer with an inorganic backbone of Si-O which is made up of repeating units of siloxane. This inorganic backbone attached to the organics group like alkyl (methyl, ethyl) or phenyl group. Depending on upon their degree of polymerization and the complexity of the organic groups, silicones can be in the form of oils, greases, rubbers, adhesives, and gel. All forms of silicone have their own usages. They have application in medical technology, industrial and manufacturing areas. Silicone significant characteristics make it suitable to be applied in different field. For instance; its thermal and chemical resistivity make it appropriate to be used as an insulator in the electrical field; its hydrophobicity has led to its application in the aerospace field and its inertness and biocompatibility improve its usage as a biomaterial in biomedical field [1]. As the pure silicone rubber demonstrates little tracking and erosion resistance, some properties of silicone rubber should be improved to extend service life and improve service efficiency. Adding filler enhances particular properties and also reduces costs [2].

These days, there is an increasing demand for products made from renewable and sustainable non-petroleum-based resources. Natural grown fibers like hemp, flax or jute are more of interest, particularly as a replacement of glass fibers. These natural fibers are cheap, have better stiffness per unit weight and have a lower impact on the environment [3]. Although natural fibers provide many advantages such as low cost, lightweight, and biodegradability over glass fiber; they have some disadvantages like low impact strength, poor thermal stability, and high moisture absorption [4]. High moisture absorbing is the major disadvantages with natural fiber decreasing their compatibility with the non-polar elastomeric matrix leading to a poor fiber-matrix adhesion. This causes low mechanical properties which is one of the drawbacks of natural fibers. Therefore, many studies have been done on modifying the fiber surface to enhance interfacial adhesion between filler particles and polymer macromolecules as well as their dispersion in the polymer matrix [5, 6]. Different chemical and physical fibers surface treatments have been used to improve the fiber/matrix interfacial adhesion [7].

Other than interface compatibility, different processing conditions can affect characteristics of the composite material and make it suitable for some specific applications. However, conventional methods to fabricate natural fiber reinforced polymer composites limit their application due to the low mechanical properties. One of the fabrication method providing enhanced mechanical properties is 3D printing of composite material which is extensively explored [8].

Currently, there are limited printable polymers including thermoplastic polymers with suitable viscosity and some photo-curable polymers. However, there is a critical need for printing soft materials in different fields like soft robotics and biomedical engineering (implants, prosthetics, and anatomical models). To improve composites printing technology, it is required to discover the desired mixing composition. Moreover, sustainable materials are promising to be developed to decrease material cost and environmental impact [9].

1.1 Research plan

This study investigates the effect of hemp fiber loading and hemp fiber surface treatment on mechanical properties and 3D printability behavior of hemp fiber silicone composites.

The main goals are to determine the desirable composition of hemp fiber/silicone and solvent to obtain enhanced mechanical properties while maintaining 3D printability. Therefore, hemp fibers were incorporated with silicone to synthesize eco-friendly and high-performance 3D printing material (Figure 1). As this material is reusable and recyclable, it is considered sustainable. These materials decrease landfill waste, reduce the need for raw materials, lower environmental impacts and energy use, and reduce air and water pollution.

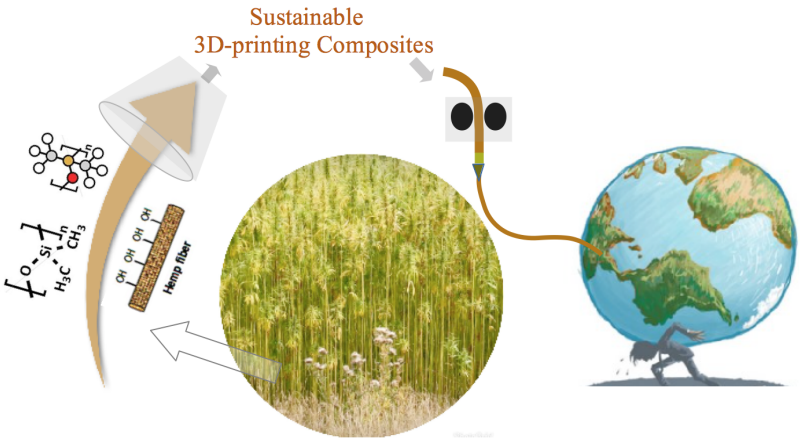

Figure 1: Sustainable 3D-printing of composites based on plant material [10].

Tensile tests were performed to obtain desirable hemp fiber loading in silicone composition to enhance mechanical properties. However, integration of hemp fibers causes major difficulties in 3D printing. This work also investigates the possibility to increase the printability of natural fiber reinforced paste-like material by modification of material viscosity, nozzle diameter, print speed, layer height. Rheological tests and physical validation were performed to determine desirable solvent and hemp fiber (wt%) in silicone composition.

The contribution of this study is to introduce a new 3D printable silicone based composite material with enhanced tensile strength. In other words, this thesis employs Direct Ink Writing (DIW)-based 3D printing to fabricate hemp fiber as a renewable

feed-stock incorporated in silicone elastomers.

1.2 Thesis outline

This work was concerned with finding a suitable composition and 3D printing parameters to make a new 3D-printable eco-friendly material.

1 . Fabrication of hemp fiber reinforced silicone rubber.

2 . Evaluation of mechanical properties to find a desirable composition.

3 . Determine 3D printing parameters for fabricating hemp fiber/silicone composition.

4 . Effect of 3D-printing on characteristics of the final product.

This thesis is divided into 5 chapters. A brief description of the chapters follows: Chapter 1 presents the introduction to the work developed. The thesis is outlined and the objective is introduced. Chapter 2 brings the literature review related to the work done. In Chapter 3, the experimental procedure is designed. The information on the experimental part of the work is detailed in this chapter. Chapter 4 brings the results found with this work and discusses the findings. The data extracted are presented, and some observations are made. Finally, the conclusions of the work and future research are stated in Chapter 5.

Chapter 2

Literature review

2.1 Composites

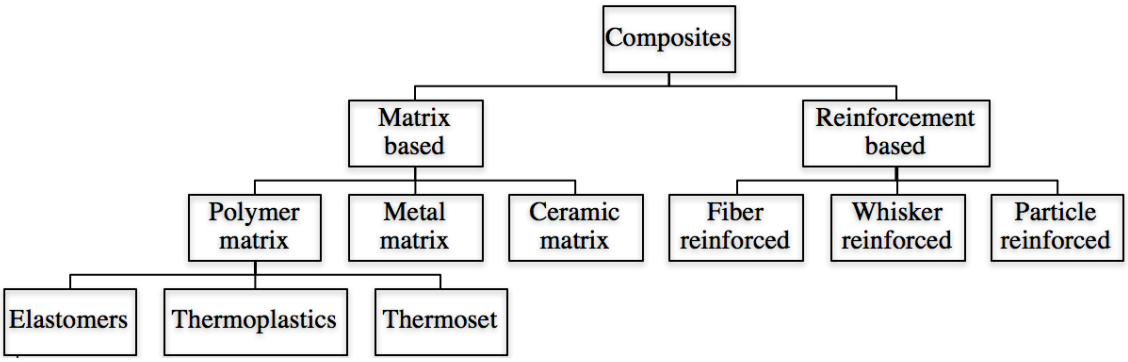

Figure 2: Different types of composites.

Composites are highly engineered manufacturing products that are designed by combining two or more constituent materials with significantly different physical or chemical properties. These constituent components are categorized as matrix and reinforcement which combined in a way that they remain separate and distinct because they don't fully merge or dissolve into one another. The reinforcement is stronger and stiffer and the matrix keeps the reinforcement which may be brittle. Composites have desirable compressibility and good tensile strength which make them versatile for a wide range of applications. Combination of different material with different characteristics results on better performance and provides the components which are called fiber reinforced composites [11].

As it's demonstrated in Figure 2 there are several different types of composites used today. One of the most common composites is fiber reinforced polymer composites. These composites are classified as either continuous (long fiber) or discontinuous (short fibers). Researches revealed that fibers alignment have a significant effect on mechanical properties. When the fibers are aligned they offer maximum strength along the direction of alignment [12].

Among different polymer, elastomers are common amorphous polymers containing polymeric chains, which are joined in a network structure possessing a high degree of flexibility and deformability. Elastomers have good damping properties making them appropriate in energy dissipation. These characteristics make elastomers desired for applications in different fields like soft robotic, automobile tires and conveyor belts,

adhesives and aircraft industry [13]. Elastomers have to be crosslinked to get rubber elasticity, and there are some elastomers demonstrating hyperplastic characteristics and behaving like thermoplastics [14].

As the pure elastomers (rubbers and thermoplastics elastomers) demonstrate little tracking and erosion resistance, some properties of elastomers can be improved to extend service life and improve service efficiency. Adding filler into elastomers can enhance particular properties and also reduce costs [3]. Different studies have been done by using different fillers like SiO_2, TiO_2, carbon black, polyester fiber, and ultra-fine calcium carbonate to induce mechanical, electrical and thermal conductivities of elastomers [15]. However, few studies have been done on the use of organic fillers to reinforce elastomers. Over the past few years, there is an increasing demand for products made from renewable and sustainable non-petroleum-based resources.

2.2 Composites of elastomers and natural fibers

2.2.1 Natural fibers

Natural fibers are obtained from plants and animals. These fibers can be obtained from leaves of plants or seed crop, from the wool of animals, and from mineral products. The most common natural fibers that can be extracted from plants are ramie, sisal, jute, sea grass flax, and hemp [16].

A wide range of natural fibers is utilized instead of synthetic and glass fiber in biocomposites. Although mechanical properties of these composites are not the same as glass fiber reinforced composites, their modest mechanical properties and biodegradability make them appropriate for applications in housing sectors, secondary and tertiary structures, automotive sector (e.g. door panels, instrument panels, armrests), textile (geotextiles and nonwoven textiles), packing materials, entertainment accessories (archery bows, golf clubs and boat hulls) [5].

Figure 3 shows different types of natural fibers. Natural grown fibers like hemp, flax or jute are more of interest, particularly as a replacement of glass fibers. These natural fibers are low cost, have better stiffness per unit weight, and have a lower impact on the environment [2].

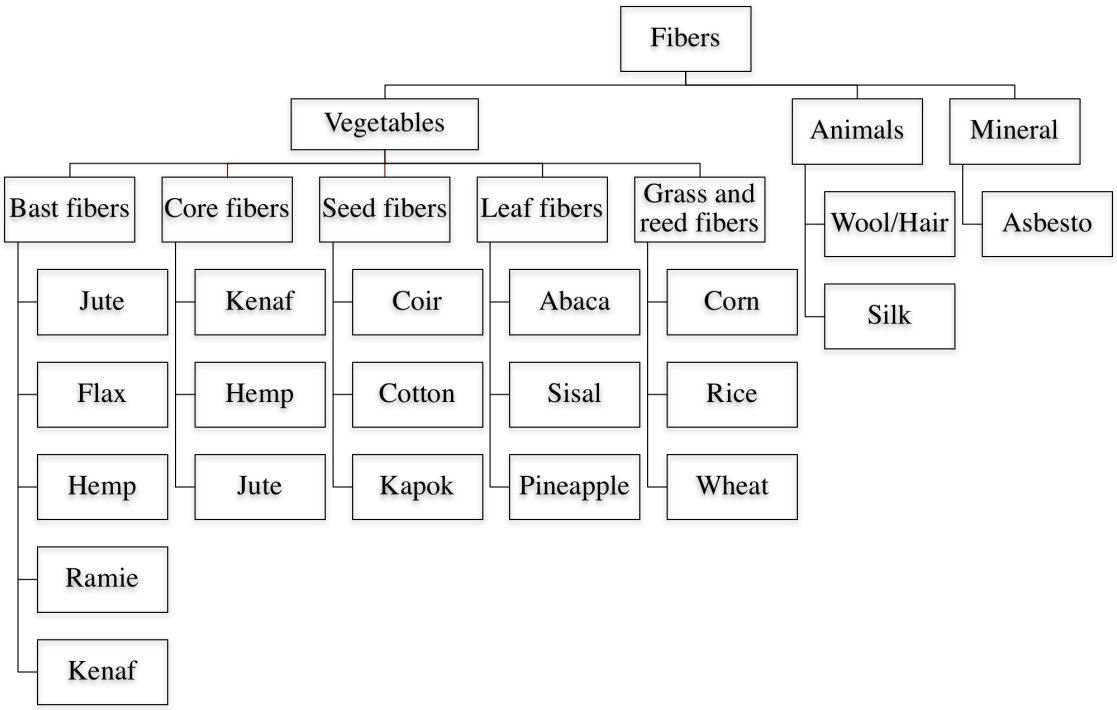

Figure 3: Different types of natural fibers.

2.2.2 Elastomeric Composites

Elastomers have excellent resilience property, but they are relatively weak in strength (Table 2). Therefore, they are commonly reinforced by glass fibers to produce the composite material. Nowadays, there is a growing interest to use natural fibers. Table 1 provides information about the most common natural fibers. The fibers have a tensile strength at a level of hundred or thousand MPa, which is $10 - 100$ times higher than the elastomers. However, they have very low elongation before breaking, which is just around $2 - 3\%$ extension of original length for most fibers. Natural fibers may not be as strong as glass fibers (e.g., 2400 MPa in tensile strength [21]), but their stiffness is comparable to glass fibers. In addition, natural fibers are green and much lighter than glass fibers. Table 2 and Table 1 show that natural fibers have higher tensile strength and stiffness compared with typical elastomers that are used as matrix. Therefore, natural fibers are used as reinforcement for elastomers [22].

To get a stronger material and transfer load from matrix, fibers should be well dispersed in matrix, and there should be a good interaction between two components

Table 1: Material properties of natural fibers.

Natural Fibers	Tensile strength (MPa)	E (GPa)	Elongation at break (%)	Ref
Jute	200-600	15-45	1.3	[17]
Bamboo	200-500	15-30	1.4	[18]
Flax	800-1500	60-80	1.2-1.6	[18]
Hemp	550-900	70	1.6	[18]
Sisal	600-800	38	2-3	[18]
Kenaf	930	53	1.6	[19]
Pineapple	200-1000	60-80	2.4	[19]
Ramie	500	44	2	[20]
Coir	220	6	15-25	[20]

[24, 25].

One of the most important issues in elastomer-based composites fabrication is that fibers should be well dispersed in the matrix. To make an appropriate interaction between elastomer matrix and fiber, physical and chemical linkage are required. Different parameters can affect fiber matrix interaction like fiber size, morphology, and surface activity [14].

The inherent hydrophilic nature of natural fibers and non-polar characteristics of the elastomeric matrix can also affect fiber/matrix interaction, and lead to non-uniformed dispersion of fibers in the matrix.

Another factor that can affect interfacial compatibility is that natural fibers absorb moisture leading to poor interaction between fibers and matrix caused by swelling and voids. The fiber/matrix interaction depends on the lignin, hemicellulose, waxes and other non-cellulose fiber sections. These non-cellulose sections avoid fiber/matrix adhesion and absorb moisture leading to fiber agglomeration trough the matrix [26, 27, 28]. Different surface treatments have been attempted to make the physical and chemical linkage between fibers and elastomeric matrix, which are presented in the next section.

2.2.3 Natural Fiber Treatment and Characterization

Different chemical treatments are applied to enhance interface interaction between the reinforcement and matrix. Many efforts have been done to modify natural fiber

Table 2: Mechanical properties of common elastomers [23].

Elastomers	Durometer (ShoreA)	Tensile (MPa)	Elongation at break%
Ethylene propylene diene	40-90	13.78	400
Styrene butadiene rubber	40-90	17.23	500
Natural rubber	30-90	24.13	600
Butyl	40-80	17.23	800
Nitrile	40-90	20.68	400
Hydrogenated Nitrile	45-90	24.13	400
Polychloroprene	40-90	17.23	500
Fluoroelastomers	55-90	17.23	200
Silicone	30-60	0.1-10	100-1100
Urethane	60-95	48.26	800
Epychlorohydrin	40-80	13.78	500

surface such that the interfacial adhesion between fibers and matrix are improved. There are review papers on different physical and chemical treatment for natural fibers including plasma treatment, heat treatment, coupling agents (silane treatment), and mercerization [29]. Here, the common methods which are mostly used in fabrication of natural-fibers-reinforced elastomers are mentioned.

Alkali treatment

The common approach which is applied in modifying the natural fiber surface to lower surface tension and to improve interfacial adhesion between natural fibers and polymer is alkali treatment or mercerization. This method increases fiber's surface roughness and thus improve the mechanical interlocking between fibers and polymer macromolecules [5, 30, 31]. Modifying natural fibers surface with aqueous sodium hydroxide (NaOH) lead to ionization of the hydroxyl group to the alkoxides. It removes a certain amount of lignin and pectin and improves the interaction between the fibers and the polymer matrix by facilitating the exposure of reactive OH groups on the fiber surface (Figure 4 (a)). Moreover, mercerization increases the amount of cellulose exposed on the fiber by increasing the number of reaction sites. Therefore, this method affects the cellulosic fibril, degree of crystallinity and extraction of lignin and hemicellulosic compounds [32]. Ray et al. [33] studied the effect of 5% NaOH treated jute fibers at different times of treatment. They revealed that after 4, 6 and

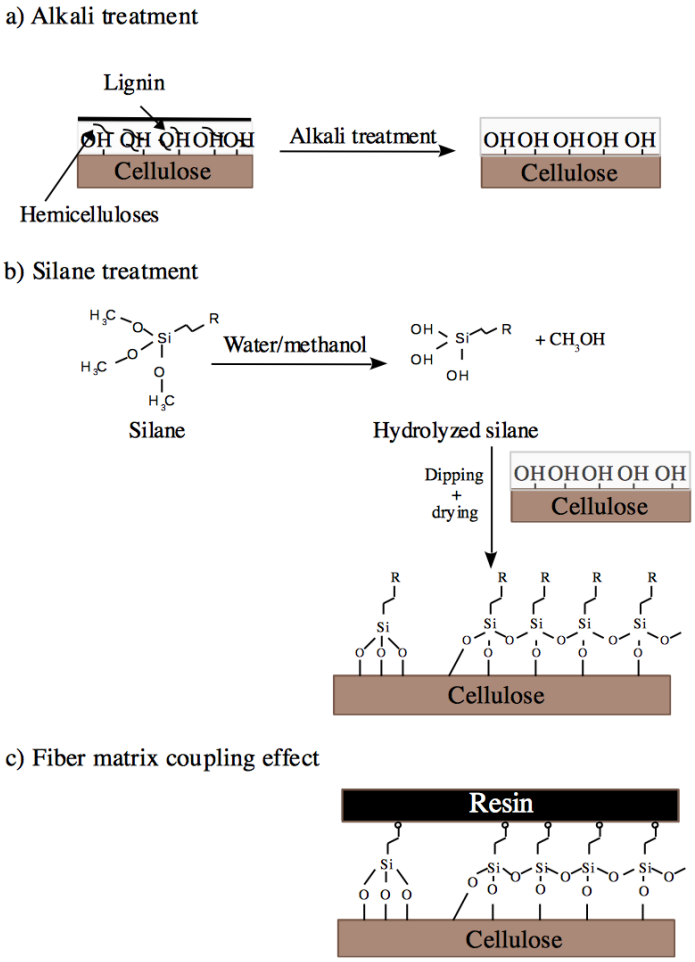

Figure 4: Effect of alkali and silane modification on a natural fiber surface [36].

8 hours of treatment the flexural modulus of jute fibers increased by 12% 68% and 79% respectively.

Gu et al. [34] studied the effect of NaOH treatment on coir fiber surfaces. The study revealed that NaOH treatment can remove all the impurities and make the surface rougher which increases mechanical bonding between fiber and matrix. Debasish et al. [35] studied the effect of alkali treatment of grass fiber on mechanical properties of the composites based on natural rubber. The results revealed that incorporation of treated grass fibers in natural rubber increased the tensile strength and elongation at break of the composites.

Silane treatment

Silane coupling agents are widely used due to their wide availability. Silane has alkoxysilane groups at one end that hydrolyze in water, and produce silanol which can react with OH reach surface. Silane as a coupling agent improves the degree of cross-linking in the interface region and increase fiber surface area for the optimization of fiber resin reinforcement [37, 38, 39].

Jacob et al. [30] did a study on mechanical properties of the sisal/oil palm reinforced natural rubber composites. It was shown that composites containing treated fibers have higher tensile strength compared with the untreated one. As it was mentioned in the previous section the removal of lignin, hemicellulose and other compounds which is resulted from alkali treatment, increase the roughness of the surface of the fibers. Moreover, alkali treatment leads to better interaction between the hydroxyl groups in cellulose and the hydrolyzed silane structure that could result in chemical bonding with the fiber surface as demonstrated in Figure 4 (b). This bonding has a significant effect on fiber matrix interaction and acts as a bridge between the cellulosic fiber and polymeric matrix [36].

2.3 Fabrication technique

Fabricating complex structure with soft material using conventional method is a tough and time-consuming process. These conventional methods are lamination casting, recractable pin casting, lost wax casting, and roto molding. These methods mostly depend on manual handling that leads to fabrication erraticism and restrictions to scientific repeatability. The restriction with lamination casting and retractable pin casting is the weak spots which limit the fabrication of complex structures. Rotomolding also has the limitation in fabricating interior parts [40, 41].

All the molding techniques limit possible geometrical shapes, complexity, and scale of the designed parts. All these limitations attract researchers' attention to additive manufacturing (AM) which needs neither a multi-step fabrication process nor human involvement. However, the most commonly used AM techniques like stereolithography (SLA), fused deposition modeling (FDM), and poly-jetting are restricted by the material utilized in the process. Currently, there are limited printable polymers including thermoplastic polymers with suitable viscosity, and some photo-curable

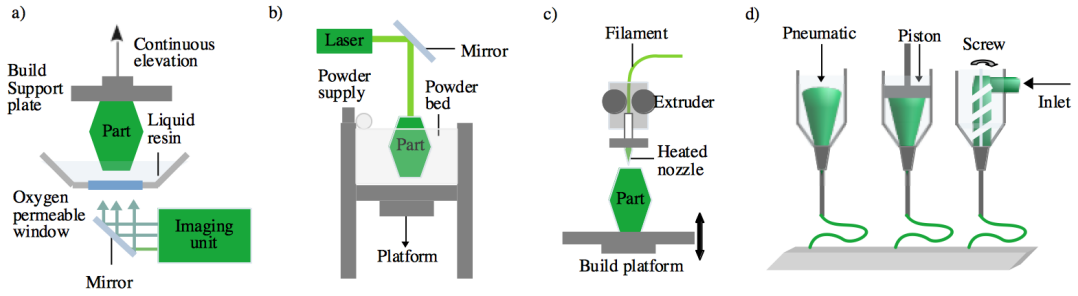

Figure 5: Different light and ink-based 3D printing methods. a)Continuous liquid interface. b) Light-based selective laser sintering of powders. c) Ink-based fused deposition modeling of thermoplastic filaments. d) Direct ink writing using viscoelastic inks[44]

polymers [42, 43].

2.3.1 Additive manufacturing

Additive manufacturing which includes a wide range of light and ink based printing gives us this opportunity to quickly convert computer-aided designs into complex 3D objects on demand. So far, the most common soft materials utilizing in printing platform are classified into three categories: photocurable resins, polymers or thermoplastic monofilaments. In 3D printing, a pattern-generating tool, either in the form of an ink-based or laser optics is moved by a computer-controlled translation stage to fabricate objects from a digital mode by depositing the constituent materials in a layer-by-layer manner. Therefore, the patterned regions build by resins, powders or inks are solidified to create the on-demand 3D form which is the concrete representations of the digital model [44].

2.3.2 3D printing of polymer matrix composites

Different printing techniques have been used to fabricate polymer composites. The most common techniques for fabricating polymer composites are stereolithography and 3D plotting, inkjet 3D printing, fused deposition modeling, and selective laser sintering (Figure 5). As it's demonstrated in Table 3 each method has its own advantages and restrictions in fabricating polymer composites. The state of starting

material, required speed, resolution, costs and required characteristics of the final components are the significant issues that should be considered in selecting printing technique [45].

Table 3: Different techniques for 3D printing polymers [45, 46, 47]

Techniques	Common Polymer Materials	Working Principle	Advantages	Disadvantages
FDM	Filament	Extrusion and depositing	Board range in materials Lower costs Less time Multi material capability High strength	Limited size Limited material Nozzle clogging Layers cause stair stepping instead of smooth surface
SLA	Liquid Photopolymer	Laser scanning and UV induced curing	High printing resolution Scalability is simple No human factor No wasted materials Biomedical applications	Limited to photosensitive resin Material limitation High cost
SLS	Powder	Laser scanning and heat induced sintering	Good strength Easy removal of support	High cost Powdery surface
3D-bioplotter	Liquid paste	Pressurized syringe extrusion, and heat or UV assisted curing	High printing resolution Soft materials capability	Low mechanical strength Slow

Polymer materials are providing different advantages like low weight, low cost, and processing flexibility which make them appropriate to be used in the 3D printing industry. However 3D printing can result in poor mechanical strength and functionality. To overcome these issues, different materials are combined together to get on-demand mechanical and functional properties. Recently, there is an increasing demand for developing 3D printable polymer composites. Different studies have been done in case of developing new materials which are compatible with available printers [45].

3D printing particle reinforced polymer composites

One of the most common composites is polymer composites reinforced by particles. Particles with low cost are used to enhance the properties of the polymer matrix. Moreover, particles in a different form can be mixed with a polymer. Therefore, it can be mixed in with the polymer in a different form, either in powder form for SLS or liquid state for SLA and easily adapt to different 3D printing processes. Table 4

Table 4: Different 3D printing methods for fabricating polymer composites reinforced by particles [45]

Techniques	**Materials**	**Enhancement in properties**
FDM	Iron/ABS Copper/ABS Al2O3/Nylon-6 Iron/PLA	Improved storage modulus and thermal conductivity Reduced coefficient of thermal expansion Reduced anisotropy of printed components
SLA	Thermoplastic elastomer/ABS Al2O3/UV cured resin	Improved dielectric permittivity and reduced dielectric loss tangent
DLP	Diamond microparticle/acrylate based resin	Improve heat transfer
SLS	Glass bead/Nylon-11	Improved tensile modulus and compressive modulus Reduced elongation at break

summarize different 3D printing method which can be employed for fabricating polymer composites reinforced by particles. Particles are utilized for improving matrix properties. It has been revealed by Kuo et al. [48] that incorporation of AL_2O_3 and SiO_2 particles improved hardness, elastic modulus, and tensile strength of polymer composites. Other studies have been done in case of using tungsten (WC) particles for improving tensile and flexural strength [49]. Castles et al. [50] fabricated diamond photonic crystal structures based on titanate/ABS using FDM technique. The results revealed incorporation of titanate particles have a significant effect on dielectric relative permittivity.

3D printing fiber reinforced polymer composites

Using fibers as a reinforcement is another common method which is employed to improve the mechanical properties of the polymer matrix. The common techniques which are applied for fabricating fibers reinforced polymer composites are FDM and direct write technique. In FDM process polymer chips are combined with fibers in a blender and then transferred to the extruder to be fabricated to the filament. In direct writing process, the fibers are combined with polymer paste and extruded out. Glass fibers and carbon fibers are the most common fibers which are used for reinforcing

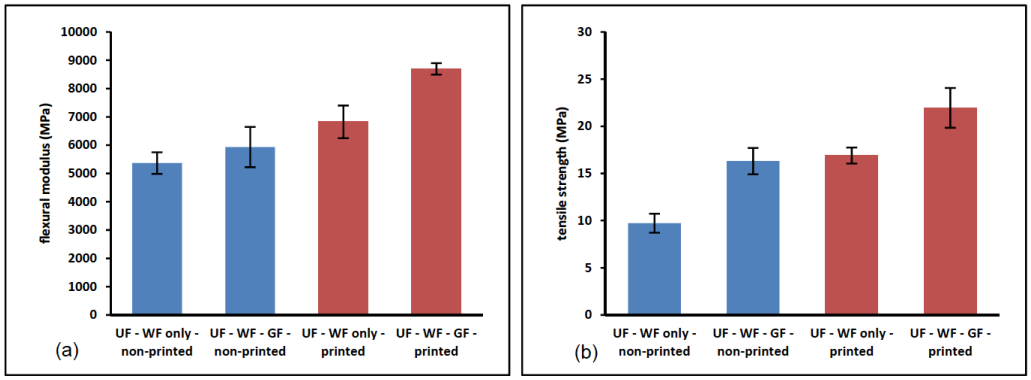

Figure 6: Comparison of mechanical properties of printed and non-printed composites [51].

polymer matrix. Two factors that have a significant effect on mechanical properties of designed composites are fiber orientation and void fraction of composites [45].

A large number of existing studies in the broader literature have fabricated polymer composite using different 3D printing methods. Ptit et al. [51] did a study on fabricating wooden composite structures with fiber reinforcement using additive manufacturing. In this study, the components from wood flour and thermoset binders were fabricated using extrusion/ deposition method. These components were achieved by extruding the paste material through a fine nozzle. It was reported that incorporation of glass fibers improved the mechanical properties of the composites. In addition, the mechanical properties of the 3D printed sample were examined and compared with the molded one. The results revealed that the 3D printed samples provide higher mechanical properties which were resulted from densification of the paste as it was extruded and deposited (Figure 6).

Micro-extrusion 3D printing techniques have also been employed in prior studies by Lewicki et al. [52] for additive manufacturing of carbon fiber filled thermoset composite material. They used direct ink writing procedure to fabricate epoxy matrix reinforced by carbon fibers and reported the highest volume fraction and aspect ratio of fibers distributed in thermoset ink. They also maximized the fiber alignment by optimizing this process using simulation and computational modeling.

2.3.3 3D printing silicone

Soft materials include a wide range of synthetic and biological materials like thermoplastic, thermosetting and elastomeric polymers, and hydrogels. These material composed of polymer chains, molecules or particles, that are moved and can be deformed under shear or other external forces [53].

The challenge with 3D printing elastomers is that this kind of materials need to be heated rapidly in order to be cured or special chemistry has to be used to cure elastomers. Recently, there is a great interest in 3D printing of silicon rubber and PDMS. 3D printing with elastomers attracted researchers attention due to its different advantages including the ability to create complex interior structures, different degrees of hardness which makes it appropriate to be utilized in different applications. The capability of silicone to be cut and stitched, making it desirable to be used for pre-surgical planning and testing [54, 55]. The current market of medical applications like prostheses or epitheses can be notably multiplied by 3D printing with silicone. 3D printing silicone has a significant impact on providing models with educational functions like the models utilizing at medical schools in biology. Currently, various 3D printing technologies are qualified to fabricate soft materials. Digital Light Processing printer was employed by Peele et al. [56] to fabricate soft actuator with a complex structure. They provided the method to successfully fabricate antagonistic actuator pairs with two degrees of freedom using photocurable elastomeric polymer. Fabrication of this design would be difficult using a mold.

Figure 7 demonstrates the complexity of the fabricated structure. One of the restrictions with Photocurable materials is that they cannot provide a wide range of properties as sealant silicone. Bastol et al. [58] employed a 3D printing technology to develop a new magnetorheological (MR) hybrid elastomer. The MR fluid was encapsulated in elastomer matrix layer by layer using 3D printing and each layer was a composite structure based on MR fluid and elastomer matrix. The results revealed the relative change in damping capability and stiffness of magnetorheological elastomer which resulted from exposure of an external magnetic field. A more systematic and theoretical analysis is required for using the 3D printed H-MRE materials in potential applications like a tunable spring-damper element. Different studies have been done in case of 3D printing silicone with different curing time, but few studies have been done in case of 3D printing elastomeric composites based on silicone and natural fibers.

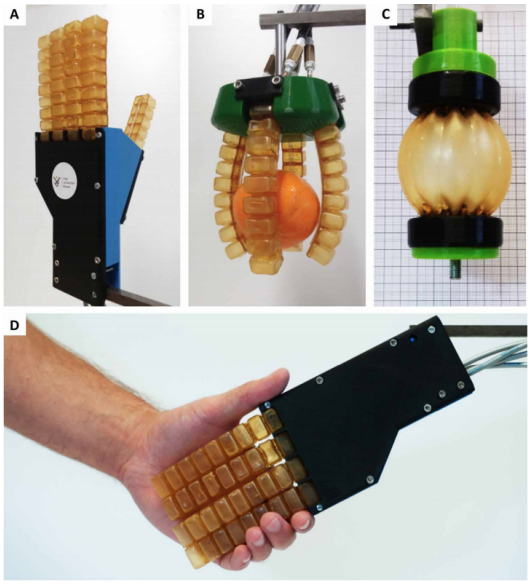

Figure 7: Four-chambered actuator [57].

The new idea is designing printable material with enhanced mechanical properties. In fact, the elastomeric composite based on silicone and natural fibers is placed in the 3D printer to print different models for different applications.

One of the most common materials which is utilized for fabricating soft actuators is Ninjaflex thermoplastic. Yap et al [59] fabricated soft actuator using a consumer 3D printer. One of the drawbacks with Ninjaflex is it cannot span large gaps.

Yirmibesoglu et al [43] did a study on the fabrication of two parts silicone material by employing custom 3D printing and extrusion mechanism with the ability to 3D print soft functional robots. They optimized print parameters such as print speed, flow rate, and temperature for fabricating two-part platinum cure silicone employing direct ink writing (DIW) technique. Then, they successfully fabricated soft robots (Figure 8) using optimized parameters.

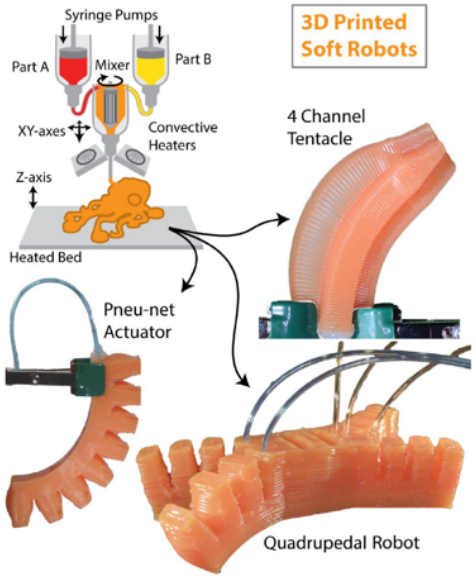

Figure 8: 3D-Printed soft robots (© 2018 IEEE)

The novelty of the following work is the type of material which can be printed. This study reports the design of new material based on hemp fiber as a renewable feedstock and silicone sealant elastomer. Multiple experiments were conducted to compare the performance differences between pure silicone and hemp fiber reinforced silicone composites.

A Paste extruder was added to a Ultimaker 3D printer. The of material properties were studied to make a printable material with enhanced mechanical properties. Tensile test was performed to compare the differences between our 3D printed dog-bone shape samples and their molded counterparts.

Chapter 3

Experimental procedure

3.1 Introduction

As it was mentioned in previous chapters, silicone is a 3D printable material, however, its low mechanical properties limit its application in the different field. In this study, hemp fibers from renewable resources used as reinforcement in silicone matrix. Hemp fibers were distributed in the silicone matrix using vacuum mixer and dog-bone shape samples were fabricated by molding technique. Different tests were performed to figure out a desirable composition which provides enhanced mechanical properties and possesses printable behavior. After finding desirable composition with enhanced mechanical properties, printability of the hemp fiber/silicon composite was investigated. This chapter describes in detail the experimental procedure followed in this work.

3.2 Material

All of the materials employed in this work were obtained from commercial sources. Untreated hemp fibers with a length ranging from 5 to 10 mm were provided by Ontario Hemp Materials company. The silicone used for the study was GE 100% silicone. 3-Aminopropyltriethoxysilane (3-APS) was purchased from Gelest Inc.

3.3 Fiber surface modification

Hemp fibers were dried in an oven and passed mesh No.40 ($420\mu m$). The length of the fibers used in this study was ranging from 0.2 to 0.4 mm (Figure 9).

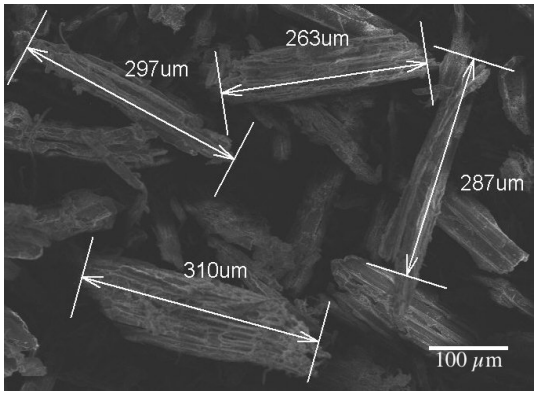

Figure 9: SEM micrographs of hemp fibers.

$$Fiber - OH + NaOH \rightarrow FibrO^{-}Na^{+} + H_2O$$

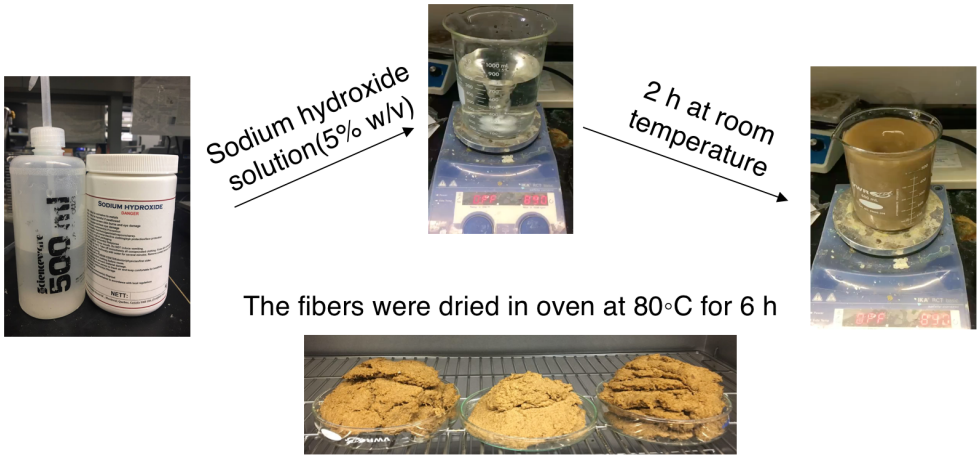

Figure 10: Surface modification of hemp fiber using alkali treatment

3.3.1 Alkali treatment

Hemp fibers were soaked in a sodium hydroxide (NaOH) solution of concentration 5% (w/v) for 2 hrs at room temperature. Fibers were further rinsed with distilled water containing acetic acid. This procedure was done two times until the pH of the rinse water reached 7, and the water no longer indicates any alkalinity. Then the fibers were air dried for two days. At the end, fibers were dried in an oven at 80 °C for 6 hrs (Figure 10). NaOH treatment provides rougher surface by removing impurities and noncellulosic parts which increase the adhesive nature of natural fibers.

3.3.2 Silane treatment

Following literature [60, 61], silane solution was made by hydrolyzing 5% (wt) silane 3-APS (weight percentage regarding the fiber) in a mixture of water and methanol (40:60 w/w). The pH of the solution was adjusted to 4 with acetic acid. The fibers were immersed in this solution for 3 hrs. Then, they were washed and air-dried for two days, and further dried in an oven at 80 °C for 12 hrs.

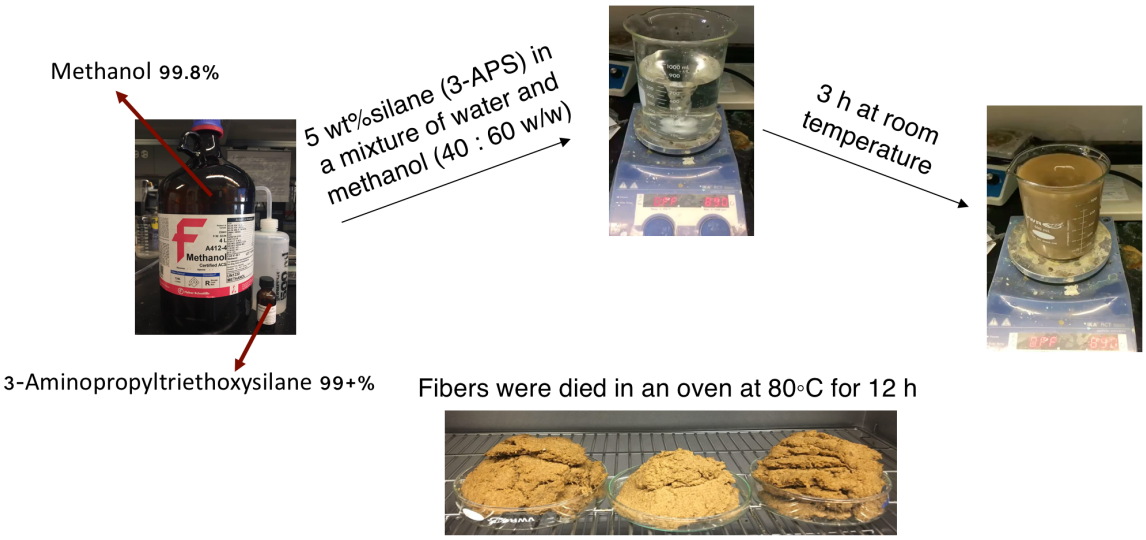

Figure 11: Surface modification of hemp fiber silane treatment

3.4 Fabricating composite based on silicone/hemp

Modified fibers were distributed in the silicone matrix using a vacuum mixer. Therefore, the fibers were dispersed in the matrix by mechanical stirring for 4 minutes. Figure 12 demonstrates the mixer which was employed for distributing hemp fibers in the silicone matrix. The duration of mixing depends on material behavior. As one component silicone starts to be cured after 4-5 minutes, the fibers were dispersed in matrix in 4 minutes. The hemp fiber reinforced silicone composites were acquired

Figure 12: Conditioning vacuum mixer ARV-200

by mixing one component silicone which cures to a tough, durable, resilient silicone rubber on exposure to atmospheric moisture at room temperature with fiber loading 10, 15, and 20 wt%. (Composites were obtained with raw fibers, alkali treated fibers,

and alkali/silane treated fibers).

3.4.1 Molding

To determine the composition with enhanced mechanical properties and investigate fibers dispersion in the matrix, dog-bone shape samples with different composition were molded. To prepare samples, a dog-bone shape ABS mold was prepared using 3D printer according to ASTM D412-16 standard which is the standard test method for Elastomers Tension. The experimental setup was established based on the principle of the molding process. The tensile samples were prepared for 10%, 15%, and 20% of hemp fiber reinforced silicone composite. The thermoset silicone composites were cured on exposure to atmospheric moisture at room temperature for 15 h to form cross-linked molecular bonds in all composites (Figure 13).

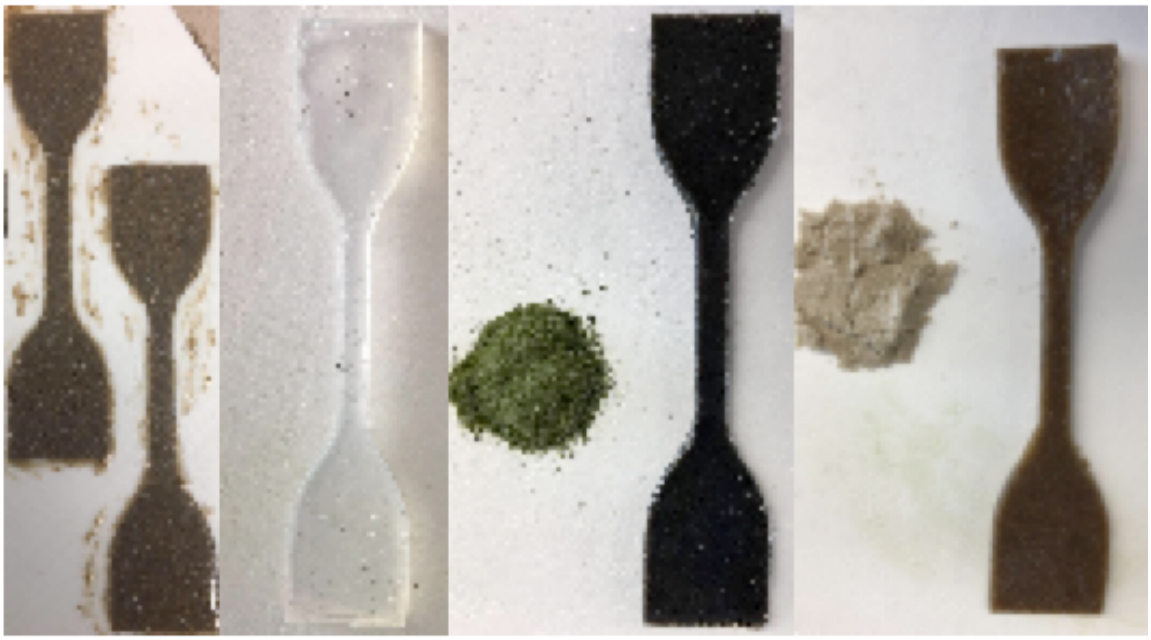

Figure 13: Molded hemp fiber reinforced silicone composites.

3.5 Silicone/hemp fiber composites characterization

To figure out the desired composition and obtain information about fiber/matrix interaction, tensile test, Fourier transform infrared spectrometry, and Scanning electron microscopy were performed.

3.5.1 Mechanical Characterization

To determine the tensile properties of the products, the tensile test was performed using tensile test machine from Hoskin Scientific company equipped with 5 kN load cell. The test was developed according to requirements of ASTM D412-06a which is the standard test methods for vulcanized rubber and elastomers-tension. The testing process was carried out at a crosshead speed of 150 mm/min a gauge length of 40 mm, and the average values of tensile strength and modulus were recorded for 10 samples of untreated, NaOH treated, and NaOH/silane treated hemp fiber silicone composites.

The test specimen for hemp fiber reinforced silicone composites were prepared in dimensions which are shown in Table 5.

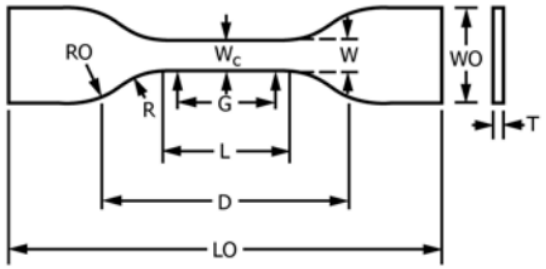

Figure 14: Tension Test Specimens for silicone

Table 5: Specimen Dimensions in (mm)

W	L	WO	LO	G	D	R	RO	T
6	33	25	115	25	65	14	25	3

The hardness was measured using Phase-II PHT-980 Durometer, Shore A scale. The tests were developed according to requirements of ASTM D2240-15 Standard

Test Method for Rubber Property—Durometer Hardness.

3.5.2 Fourier transform infrared spectrometry (FT-IR)

Infrared spectroscopy is a helpful analytical method for investigating the structural identification or confirmation of identified or unidentified product. An infrared spectrum allows to easily discover the presence of significant functional groups. FTIR study of the untreated, NaOH treated, and silane treated hemp fibers were done by using a FTIR machine (Nicolet 6700 / Smart iTR) to determine the changes in functional groups on the fiber surface. All the spectra where recorded in a range of $4000cm^{-1}$ to $500cm^{-1}$.

3.5.3 Scanning electron microscopy

To analyze the fracture surface of hemp fiber reinforced silicone and to visualize the effect of alkali and silane treatment, Scanning electron microscopy (SEM, Hitachi, S-3400N) was utilized. The voids, microstructures, and interfacial interaction of fiber and matrix were determined using SEM at voltage 5 KV, pressure 50 Pa, and at a focusing distance of 5 to 10 mm, for magnification of up to 1000X used in this study. In order to establish effective conductivity for examination, the fracture surfaces of tensile samples were gold sputtered.

3.6 3D printing

After determining the desired composition, the printability of the silicone/hemp fiber composites was evaluated. For 3D printing hemp fiber/silicone composite the Discov3ry paste extruder was employed. This extruder can be easily added to any existing 3D printer. The Ultimaker line is our printer of choice as it's open source, very well engineered, and extremely reliable. The Discov3ry provides the opportunity for printing both plastic and paste materials. This printing technique allows going beyond printing plastic filament and instantly print with different types of materials like silicone easily using design slicing software. Hemp fiber reinforced silicone composite was loaded into a syringe cartridge, and the Discov3ry Extruder system forced the paste through a feed tube. The material was injected through the nozzle and

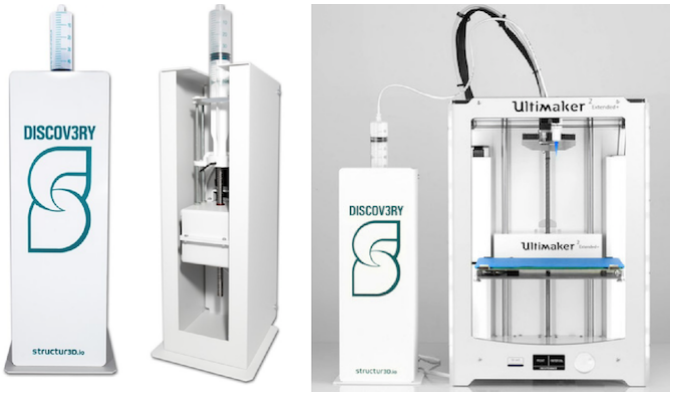

Figure 15: Ultimaker and the Discov3ry paste extruder [62].

deposited on platform layer by layer. This study investigated, the effect of different parameters on 3D printing of hemp fiber reinforced silicone composites.

3.6.1 Printability assessment method

Printable ink must provide a number of significant requirements to be processed with DIW 3D printing method. This study investigated the desirable condition to address printability issues. Therefore, this work proposed a two-step evaluation to characterize material printability. The first evaluation step which is demonstrated in Figure 16 was studying rheological properties. In other words, material properties were studied before, during and after being extruded in 3D printer. The second step (Figure 16) was extruding material manually to find the ability of the material to form continuous flow, rather than a droplet, and to validate rheological results.

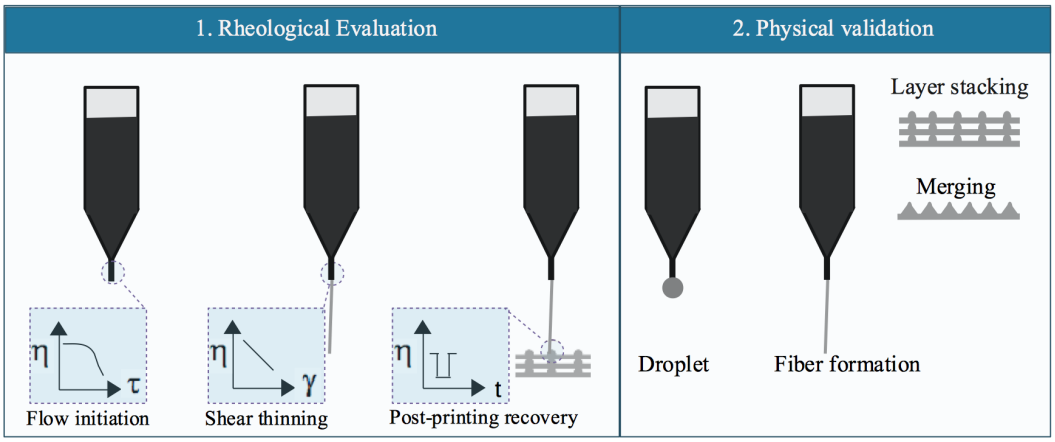

Figure 16: Schematic of the proposed research method to determine printability of the designed material.

3.6.2 3D printing parameters

Effect of viscosity

Incorporation of fibers can affect curing time and makes silicone unprintable. To solve this problem, mineral spirit was used as a solvent (Figure 17). The significant issue that has to be considered in case of 3D printing paste material is constant flow which can be examined effectively by hand. Therefore, the silicone/Hemp fiber composition incorporating a range of solvent concentrations were extruded manually. The flowing of designed material was studied and compared to the 0 (wt%) solvent.

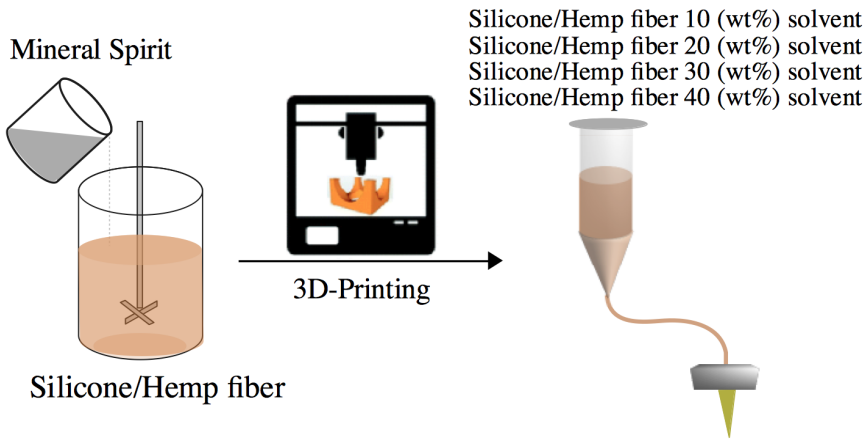

Figure 17: Dissolving silicone/Hemp fiber in solvent.

Effect of nozzle diameter

The internal nozzle diameter has a significant effect on the way that the material is being extruded. The velocity of the extruded silicone will be different for different nozzle size. The smaller the diameter the higher the velocity which results in curling of extruded silicone. In this study, we printed silicone using the parameters which were reported in previous works. The employed 3D printing parameters for fabricating silicone are demonstrated in Table 6 [63]. For fabricating silicone reinforced by hemp fibers we changed the 3D printing parameters. As fibers got stock in 0.84 mm nozzle, a bigger nozzle was used for fabricating hemp fiber reinforced silicone composites. Therefore, a 1.54 mm nozzle was found appropriate to print hemp fiber reinforced silicone. The larger the fibers, the bigger the nozzle diameter.

Table 6: Optimized 3D printing parameters for fabricating silicone

Material	Layer height (mm)	Infill density (%)	Print speed (mm/s)	Travel speed (mm/s)	Nozzle diameter (mm)
Silicone	0.3	100	10	120	0.84

Effect of print speed

The challenge with 3D printing elastomers is that this kind of materials requires a specific chemical reaction. For instance, the one component silicone is cured to durable tough silicone rubber on exposure to atmospheric moisture. Moreover, It takes longer for silicone to get cured in comparison with thermoplastics (like ABS and PLA). The printing speed can significantly affect the initial adhesion to the building platform [54, 55].

In most cases, there should be a balance between the printing speed and consistency of feeding. As it's shown in Table 6, the print speed which was employed to fabricate silicone is 10 mm/sec, that should be higher than can be used with viscose material. The viscosity of silicone/hemp fiber composition was decreased by dissolving the material in the solvent at the beginning, but over curing time the solvent was evaporating and the material was getting more viscose. Therefore, to get consistent flow over whole 3D printing process, print speed was decreased. Different print speeds were tried, and 8 mm/sec was chosen as a suitable print speed for fabricating hemp

fiber/silicone composition.

Effect of layer height

As it was mentioned 1.54 mm nozzle was selected for 3D printing hemp fiber silicone composites. It has been reported that the layer height should not exceed 80% of the nozzle diameter [64]. For the 0.84 mm nozzle, the layer height is 0.3 mm, and it should not exceed 0.67 mm. As 1.54 mm nozzle was selected for printing silicone hemp fiber, the layer height should not be exceeded 1.23 mm. Different layer height, ranging from 0.3 mm to 1 mm were tried, and 0.5 mm exhibited better results compared with others.

The parameters nozzle diameter, layer height, infill density, and print speed were determined by 3D printing dog-bone shape sample to acquire the good model quality. Table 7 demonstrates the 3D printing parameters for 3D printing hemp fiber reinforced silicone composites.

Table 7: 3D printing parameters for fabricating silicone/hemp fibers.

Material	Layer height (mm)	Infill density (%)	Print speed (mm/s)	Travel speed (mm/s)	Nozzle diameter (mm)
Silicone	0.5	100	8	120	1.54

3.6.3 Step 1: Rheological evaluations

MCR301 rheometer (Anton Paar) was employed to measure the rheological properties of the silicone and hemp fiber reinforced silicone. A 25 mm parallel plate with a measurement gap of 1 mm was used. One of the goals in this study is to determine whether hemp fiber reinforced silicone could be fabricated using 3D extrusion printing. In order to understand the printability of silicone/hemp fiber, it is essential to monitor the rheological behavior of all experimental samples during processing. In this study, the following three rheological experiments at room temperature were carried out in order to find solvent concentration which provides 3D printability without changing material characteristics; (1) For all experimental samples containing different solvent concentration, a shear stress ramp ranging from 0.01 to 100 Pa was applied, to determine the yield point, indicating the point at which the material first

started to flow. (2) Rotational shear viscosity measurements were done in flow mode in a range of 0.01 to $100s^{-1}$, to investigate the shear thinning properties of the materials. (3) To determine the materials recovery behavior after exposure to shear rates, the rotational recovery behavior were performed by applying a low shear rate of $0.01s^{-1}$ for 200s, following by high shear rate at $100s^{-1}$ for 100 s and at the end a low shear rate of $0.01s^{-1}$ for 200 s. All these measurements were used to characterize materials and select a suitable candidate for 3D printing.

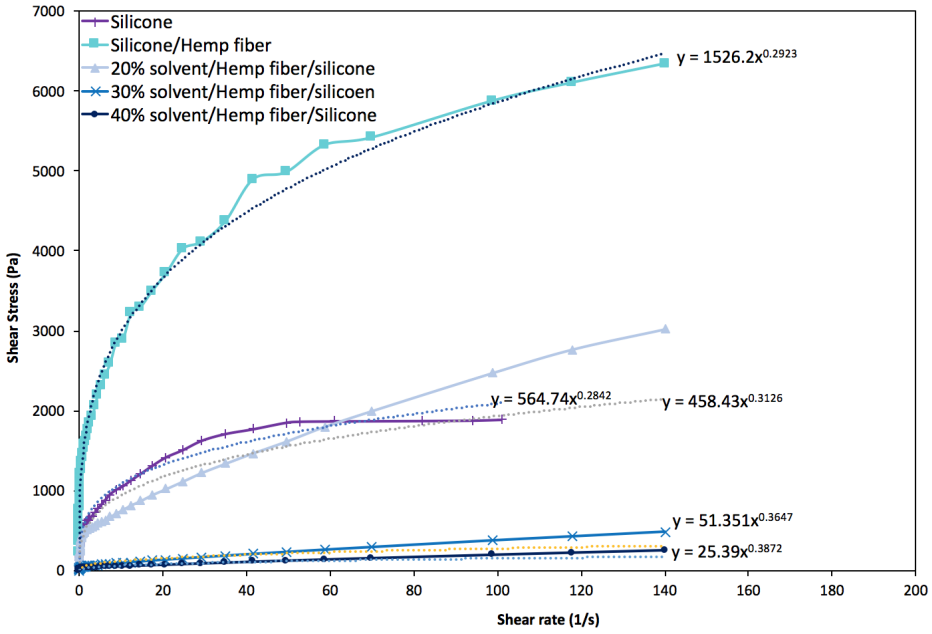

Figure 18: Shear stress-shear rate results for all experimental samples

Calculation of shear rate in nozzle

For some rheological measurements to simulate condition inside the nozzle, it was required to know shear rate inside the nozzle. Shear rate for shear thinning material calculated was via the following equation [65, 66];

$$\gamma = \frac{3n+1}{4n}\frac{32\dot{Q}}{\pi D^3} \tag{1}$$

Where D is the nozzle diameter, Q is the flow rate. n is the Power Law coefficient derived from the Power Law equation [67];

$$\sigma = k\gamma^n \tag{2}$$

The behavior of each sample was characterized by fitting the Power Law equation to the shear stress-shear rate rheology plot for each material. Figure 18 demonstrates the shear stress-shear rate graphs. The coefficients n and k were calculated and are shown in Table 8. These coefficients were employed to predict and analyze the condition present in the needle.

Table 8: K and N coefficients for all experimental samples.

Sample	K	N
Silicone	564.74	0.2842
Silicone/Hemp fiber	1526.2	0.2923
Silicone/Hemp fiber/20(wt%) solvent	458.43	0.3126
Silicone/Hemp fiber/30(wt%) solvent	51.351	0.3647
Silicone/Hemp fiber/40(wt%) solvent	25.39	0.3872

The calculations revealed that the shear rate inside the nozzle is around $100s^{-1}$ for all experimental samples (Table 9). In recovery test behavior to simulate the situation inside the nozzle the shear rate of $100s^{-1}$ was applied to all samples.

Table 9: Shear rate inside nozzle.

Sample	3n+1/4n	Flow rate (mm^3/s)	Shear rate (s^{-1})
Silicone	1.62	2.52	70.15
Silicone/Hemp fiber	-	-	-
Silicone/Hemp fiber/20(wt%) solvent	1.54	23.21	99.68
Silicone/Hemp fiber/30(wt%) solvent	1.43	26.04	103.85
Silicone/Hemp fiber/40(wt%) solvent	1.39	30.80	119.39

3.6.4 Step 2: Physical validation

To ensure printability of the designed material, and confirm rheological measurements results, this step was performed. All the experimental samples containing different solvent concentrations were separately loaded into syringes' barrel and pressure was applied manually to syringes' plunger. Then, the material flow was observed to discover the composition which had the capability to form a continuous flow. Moreover, honeycomb structures were 3D printed to study material capability to keep its shape after being deposited on the surface.

3.7 Gripper fabrication and testing

To demonstrate the application of additively manufactured hemp fiber reinforced silicone in soft robotic two simple grippers were fabricated. The grippers were designed (19) and fabricated with pure silicone and silicone/hemp fiber and the resistance of the silicone gripper was compared with it's silicone/hemp fiber gripper counterpart.

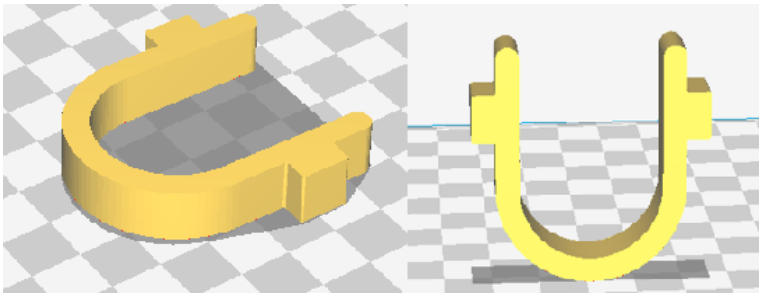

Figure 19: Designed gripper.

3.7.1 Grip Force Measurement

To quantify the grip force and soft gripper's interaction with objects, a flexible force sensor was employed. The flexible film pressure sensor DF9-40 (0-500 g) utilized to determined grip strength. This flexible force sensor was connected to a data acquisition system which is demonstrated in Figure 20.

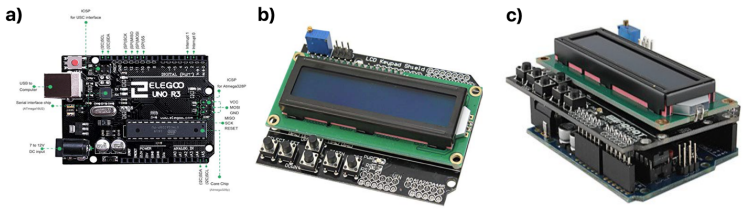

Figure 20: a):Arduino official original UNO R3 microcontroller control board with data line. b): LCD shield module display V3 for Arduino UNO R3.

The flexible sensor was powered by an on-board battery and records data to memory on the data acquisition board. The data was downloaded to a computer via a USB cable after the experiments have been conducted (Figure 21). Different ways can be employed to incorporate Flexiforce sensor in application. One way is to integrate it into a passive linear circuit to obtain an output voltage that is a fraction of its input

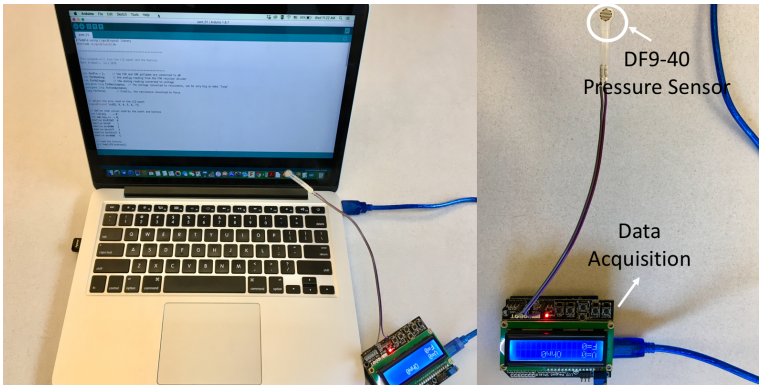

Figure 21: Force measurement device

voltage. This circuit employs an inverting operational amplifier arrangement to yield an analog output based on the sensor resistance and a fixed reference resistance (RF). An analog to digital converter was utilized to convert this voltage to a digital output. Figure 22 shows a voltage divider circuit which is employed in this study.

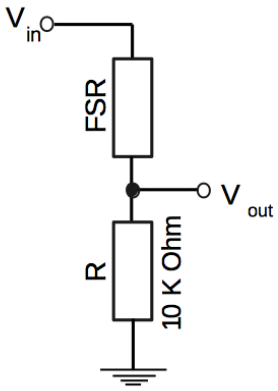

Figure 22: A simple voltage divider.

For conditioning the sensor, different weights were placed on the sensor. A significant issue should be considered is the interface between the test subject and the sensor. The whole area of the sensor should be treated as a single contact point. Therefore, the applied force should be distributed consistently across the area. If the load distribution changes over the sensing area, readings may vary slightly. For this reason, each voltage output was read after the sensor stabilized.

The graph below shows a correlation between voltage and weight. This graph was used to determine the gripper force. To ensure accurate and repeatable voltage readings, this test was repeated 10 times.

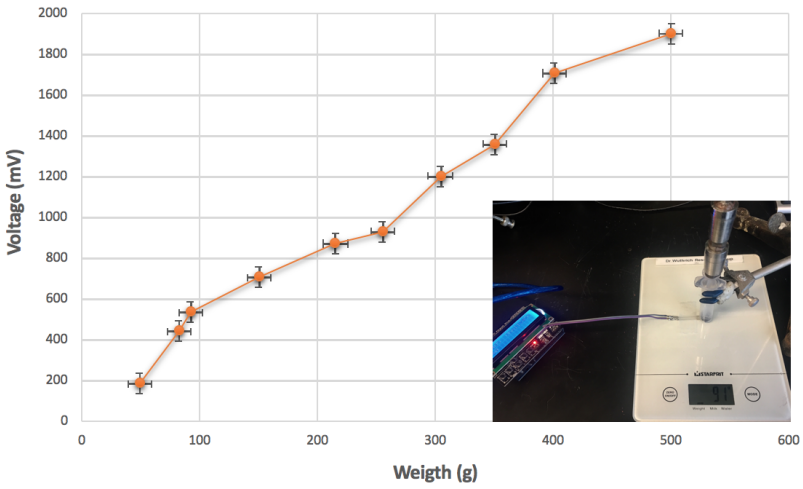

Figure 23: Voltage as a function of weight.

Chapter 4

Results and discussion

4.1 Introduction

The main focus of this study is to determine the desirable composition of hemp fiber/silicone to provide enhanced tensile strength while maintaining 3D printability. Therefore, tensile strength tests were performed on different samples to evaluate the effect of fiber loading and surface treatment on mechanical properties. FTIR spectroscopy and post-fracture image analysis (SEM) were performed to explain the enhancement of mechanical properties.

After determining the desired composition, the printability of the silicone/hemp fiber composites with different solvent concentration were evaluated with rheological evaluation and physical validation. In addition, example applications of the enhanced hemp fiber/silicone composite were demonstrated by fabricating gripper and honeycomb structure. This chapter provides detail results and discussions for each experiment.

4.2 Effect of fiber loading and chemical treatment on mechanical properties

The first goal of this study is investigating the effect of hemp fibers on mechanical properties of silicone matrix. Different factors affect tensile strength of fiber composites. Two factors are investigated; Fiber loading and the interfacial interaction between fiber/matrix.

4.2.1 Tensile Strength and Modulus of molded Composites

Figures 24 and 25 demonstrate the tensile strength and young's modulus for different compositions of untreated, alkali treated, and silane treated hemp fibers reinforced silicone composites. It is illustrated that with increasing treated hemp fiber content in the silicone matrix the tensile strength and modulus are also increasing. The incorporation of 10%, 15%, and 20% of hemp fibers, increased tensile strength by 51%, 61%, and 68% respectively and increased tensile modulus by 86%, 89%, and 94% respectively compared with pure silicone. This is explained by the fact that the applied stress is distributed to the hemp fibers by the silicone matrix. The effective and uniform stress distribution is also dependent on fiber loading. Hence, the composite with higher fiber loading tolerates higher load before failure in comparison with lower fiber loading and unreinforced silicone.

In other words, in silicone/hemp fiber composites, hemp fibers act as a carrier of load and stress which results in uniform force distribution, therefore, the higher the fiber loading the more enhanced the mechanical properties.

The incorporation of 10%, 15%, and 20% of silane treated hemp fiber in silicone composites improved tensile strength by 14%, 27 %, and 29% respectively, and tensile modulus by 37%, 54%, and 71% respectively, compared with untreated hemp fibers reinforced silicone composite.

As untreated fibers are covered by wax and contamination, there would be poor adhesion between hemp fiber and silicone matrix. Consequently, the stress cannot be transferred from matrix to fiber. In contrast, the significant increase in tensile strength of silane (3_AMPS) treated hemp fiber reinforced composites is due to a better interfacial interaction between fiber and matrix. The improvement in fiber/matrix interaction is ascribed by, enriched roughness on the surface of the fibers, and chemical

bonding between functional groups of polysiloxane and functional groups of silicone.

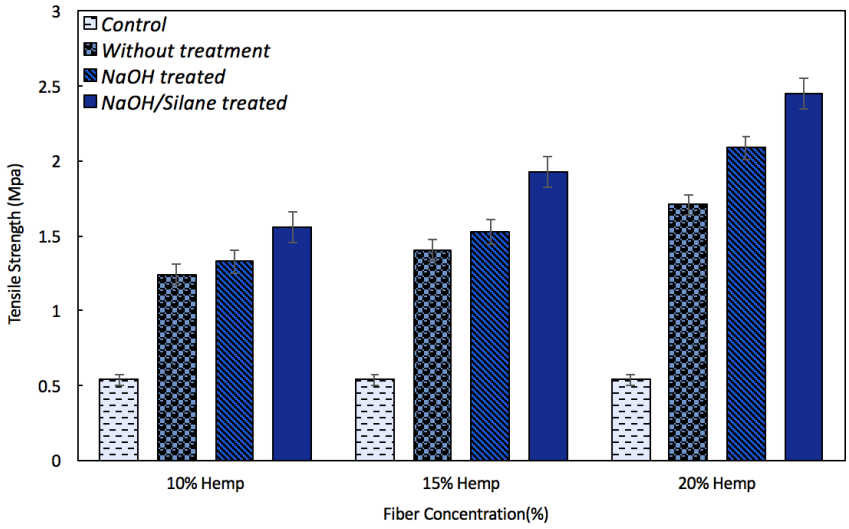

Figure 24: Tensile strength of molded hemp fiber reinforced silicone composites.

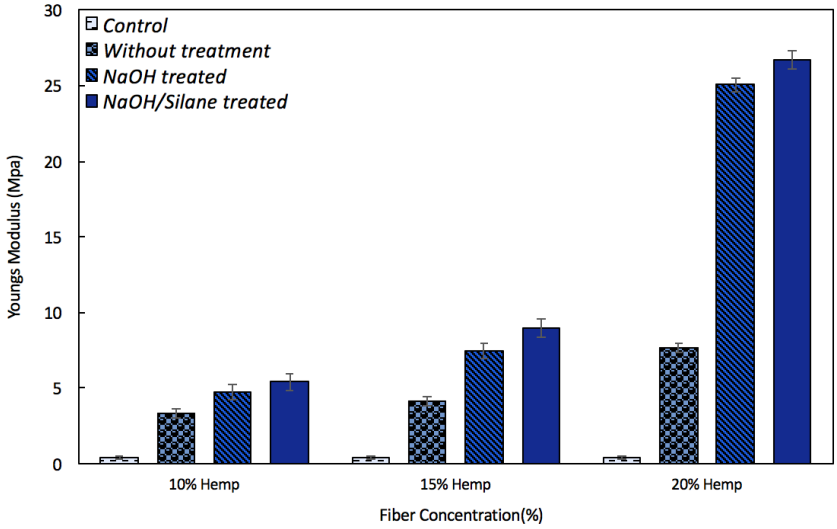

Figure 25: Young's modulus of molded hemp fiber reinforced silicone composites.

4.2.2 Hardness of molded Composites

Two parameters that can affect hardness of hemp fiber reinforced silicone are fiber concentration and fiber/matrix interaction. Figure 26 shows the hardness of silicone composites infilled by untreated and NaOH/silane treated hemp fibers. The results show that the hardness of hemp fiber reinforced silicone composites increased by increasing fiber concentration. This is due to the fact that the incorporation of fiber improved crosslink density which increased hardness and stiffness of Silicone matrix.

It is clearly evident that silicone composites incorporating treated hemp fibers provided higher hardness which was due to appropriate interface interaction between fibers and matrix.

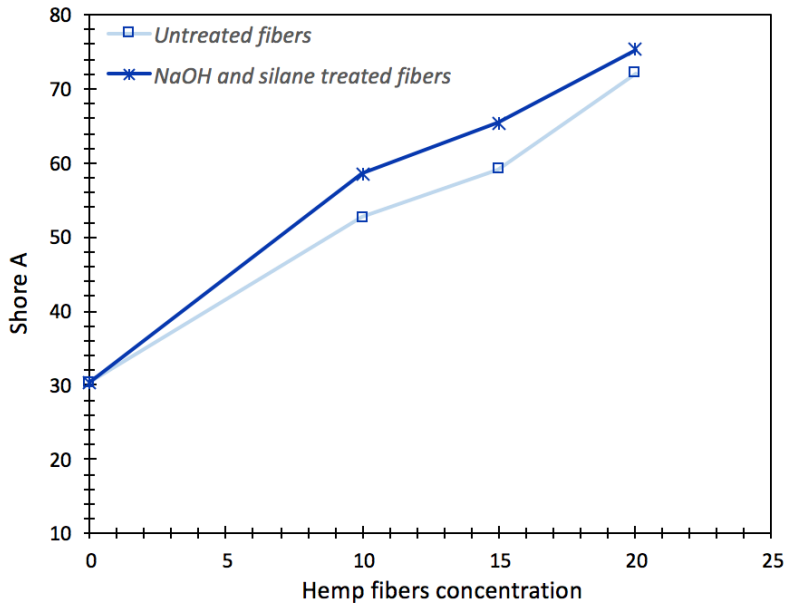

Figure 26: Hardness of molded hemp fiber reinforced silicone composites.

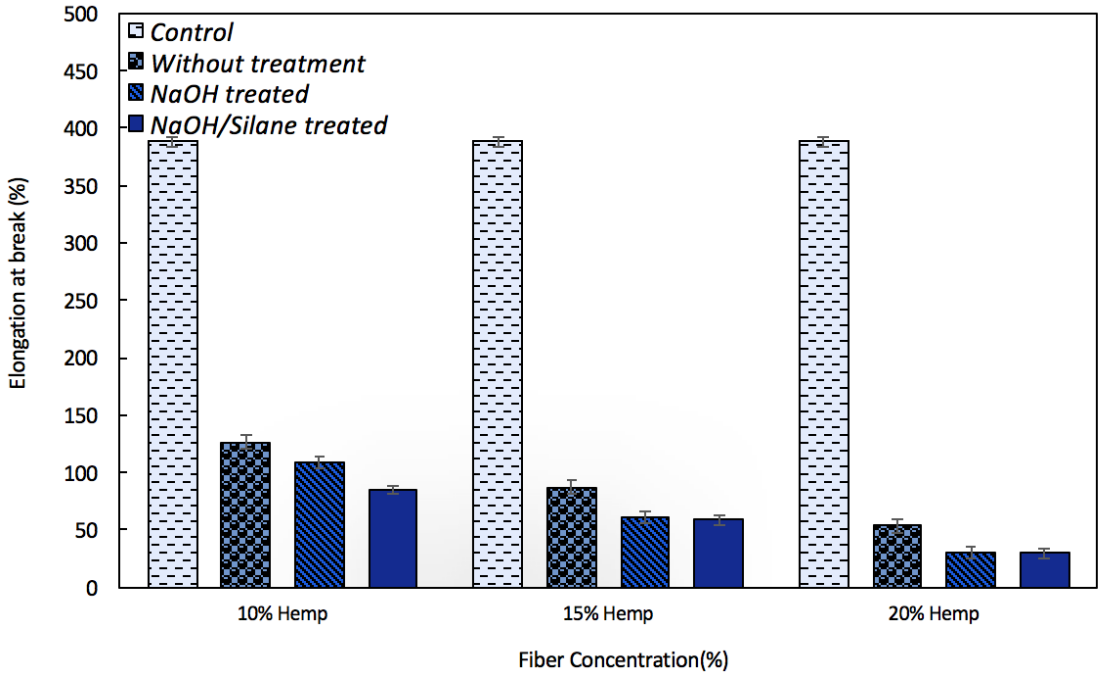

Figure 27: Elongation at break of molded hemp fiber reinforced silicone composites.

Figure 27 shows the effect of fiber incorporation on elongation at break. As it was expected the elongation at break of composites decreased by incorporation of fibers. The higher the fiber content, the higher restriction for molecular motion, resulting in lower break resistance. The incorporation of 20% NaOH/silane treated hemp fiber in silicone increased the tensile, and young's modulus by 29%, 71%, respectively. However, the elongation reduced by 44% which indicates that 20% fiber loading makes silicone more fragile compared to untreated hemp fiber silicone composite. On the other hand, 15% NaOH/silane treated hemp fibers displayed 27% and 54% enhancement in tensile and young's modulus while it showed 30% reduction in elongation compared to pure silicone. Therefore, the composition containing 15% NaOH/silane treated hemp fibers was chosen as a suitable candidate, and all the experiments were done based on this composition.

FTIR and post fracture image analysis (SEM) were performed to demonstrate enhancement in chemical and mechanical interaction between fibers and matrix.

4.2.3 Interfacial interaction between fiber/matrix (FTIR)

The existence of modifications in the chemical bonding in the NaOH treated, Silane treated and untreated hemp fibers were determined by FTIR spectroscopy. Figure 28 demonstrates spectra of treated and untreated hemp fibers. The peaks around 3280 and 3380cm^{-1} confirm the presence of hydrogen bonded O-H stretching present in aliphatic or aromatic alcohols in the fiber components. The increase in the absorption Of O-H region after NaOH could be due to the possible withdrawal of hemicellulose and lignin which results in increasing number of exposed O-H groups from the surface of the fibers. The peak around 2859 and 2920cm^{-1} corresponds to C-H stretching vibration from aliphatic saturated compounds, like aliphatic moieties in cellulose and hemicellulose. The peak 1706cm^{-1}, results from vibrational stretching of carbonyl groups (C=O) which is related to hemicelluloses and lignin. As it is illustrated, the reduction in the peak intensity around 1706, is due to the removal of lignin and hemicelluloses after alkali treatment. Moreover, the peak intensity around 1235 ascribed C-O stretching of acetyl groups in the hemicellulose diminished by alkali treatment. The appearance of the peak around 1100 is corresponding to asymmetric stretching of Si-O-Si, and Si-O-cellulose. The intensity of the peak around 1100 increased after silane treatment.

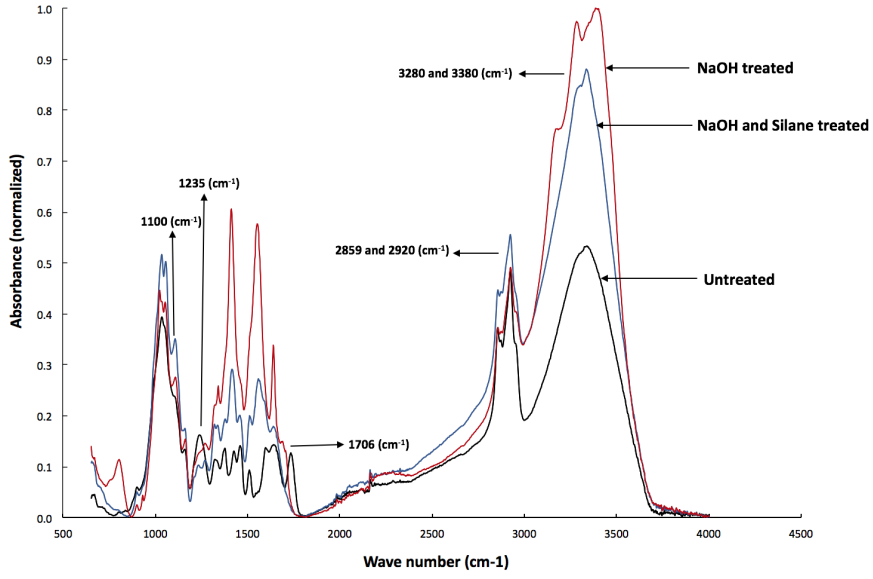

Figure 28: Fourier transform infrared (FTIR) spectrum for treated and untreated hemp fiber.

Table 10: IR absorption of functional groups.

Functional groups	Absorption location (cm^{-1})
O-H stretching	3280 and 3380
C-H stretching	2859 and 2920
C=O stretching	1706
C-O stretching	1235
Si-O-Si and Si-O-cellulose	1100

These adjustments are required for natural fibers used as reinforcement for polymer matrix. The polysiloxane has higher functional groups compared with fiber surface, which can easily react with the functional group of polymer matrix and established stable bonds. It can be concluded from the results that the silane coupling agent was grafted on the fiber surface. The findings of this experiment are in agreement with previous studies [68, 69, 70, 71]. Table 10 lists the locations of absorptions produced by functional groups.

4.2.4 Morphology of the hemp fibers (SEM)

Figure 29 demonstrates the surface micrographs of untreated and alkali treated hemp fiber. It is clearly evident that the surface of raw hemp fibers differs from NaOH treated fibers in roughness (Rz). SEM images demonstrate that the surface of untreated hemp fiber is smoother than the surface of alkali treated fibers, leading to weak interfacial bonding with polymer matrix, however, the alkali treatment increased the roughness of fiber surface (Rz). In fact, alkali treatment made fiber surface rougher due to removal of noncellulosic parts like pectin, wax, and lignin. This rough surface facilitates mechanical interlocking between fiber and silicone matrix. Therefore, alkali treatment increases the effective surface area available of contact with the matrix and improves the possibility of load transfer from matrix to fibers.

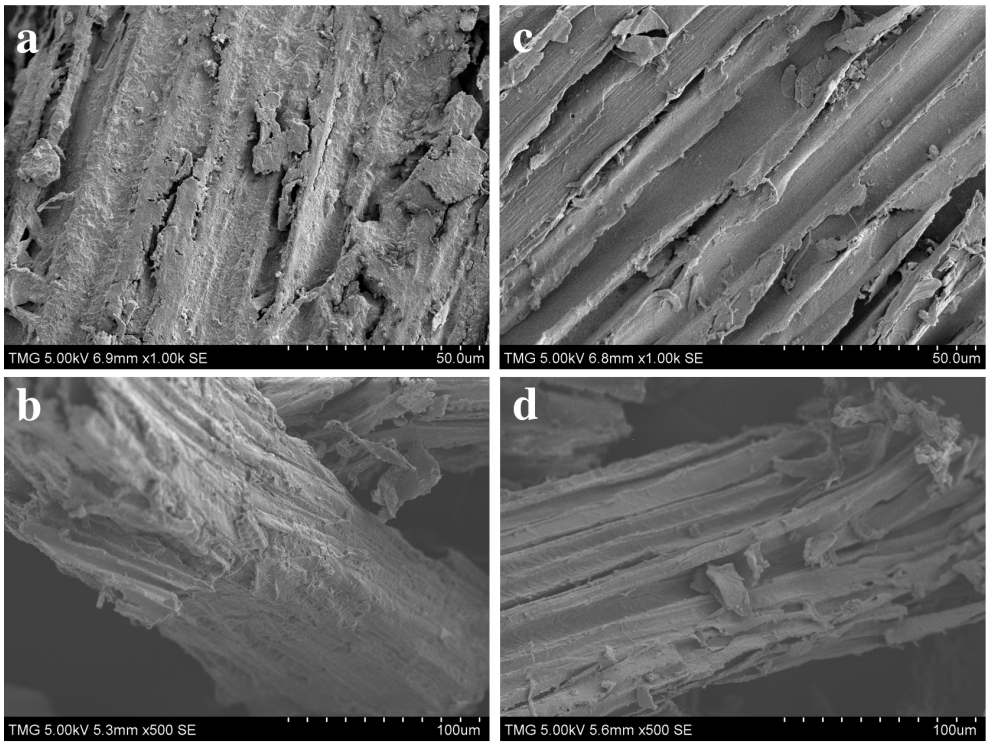

Figure 29: SEM images of (a),(b) untreated (c),(d) alkali treated hemp fibers.

4.2.5 Effect of chemical treatment on interaction between fiber and matrix

To investigate the interaction between fibers and matrix scanning image analysis was performed giving essential information about fibers distribution in matrix, and the adhesion between two phases. Figure 30 represents SEM images of the impact fracture surface of the composites. This figure illustrates, that untreated fibers were presented in the form of multi-fibers instead of distributing uniformly.

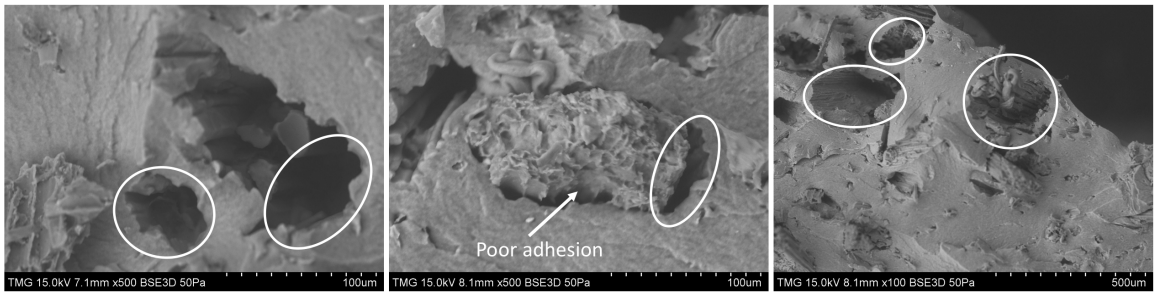

Figure 30: Fractured surface of untreated hemp fiber reinforced silicone.

It's demonstrated that there is poor adhesion between untreated fiber and matrix which led to appearance of pull-out holes in composites. Indeed, there is no physical contact between both components in the interfacial region.

Figure 31 demonstrates the effect of NaOH/silane treatment on interface interaction between hemp fiber and silicone matrix. As it's demonstrated fibers are totally covered by the matrix and there is no void between the two phases. In fact, the interfacial adhesion is affected by the changes of surface topography, because the higher the roughness of alkali treated fiber the better mechanical interlocking between fiber and matrix. Therefore, chemical treatment improved the adhesion at the interface leading to higher mechanical properties. This results concur well with other studies [72, 73] and also confirms our previous findings.

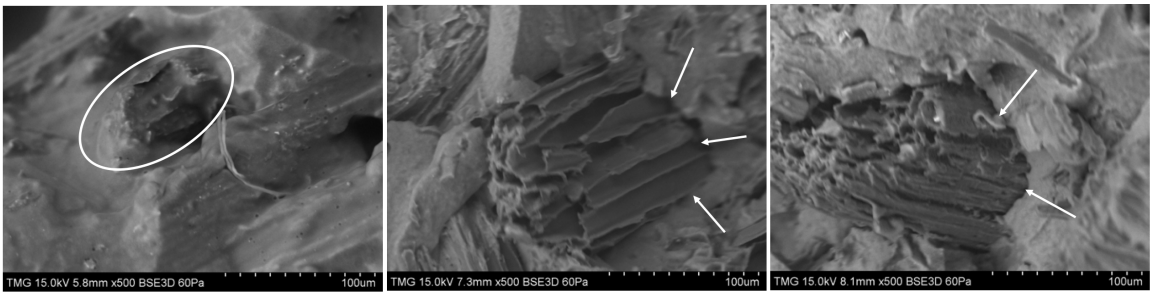

Figure 31: Fractured surface of NaOH/silane treated hemp fiber reinforced silicone.

4.3 Printability assessment

Extrusion of material with continuous flow and the ability of the fabricated sample to keep its shape without flowing are the two essential requirements for 3D printing. Silicone is a printable material. However, incorporation of hemp fibers in silicone will increase its viscosity which leads to unprintability behavior.

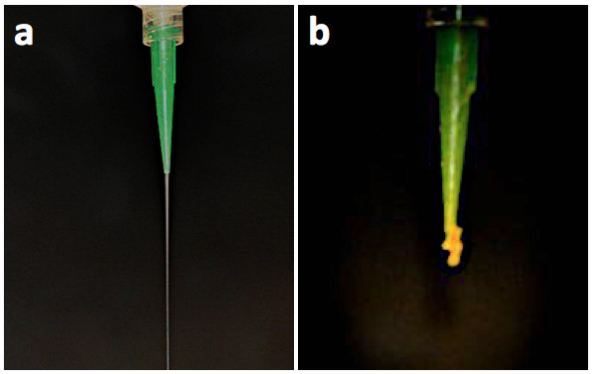

Figure 32: Effect of fiber incorporation on material flow; a) Pure silicone b) Silicone/hemp fiber.

Figure 32 (a) demonstrates the behavior of silicone after extrusion. The material flow was consistent and kept its shape without breaking and detaching which confirmed the printability of pure silicone. Distribution of hemp fibers through silicone matrix changed silicone behavior and resulted in an unprintable behavior as shown in Figure 32 (b). Different solvent concentrations were used to reduce the viscosity of the composition, and bring back printability behavior. Therefore, rheological evaluation and physical validation were performed to determine the printable composition without changing material characteristics.

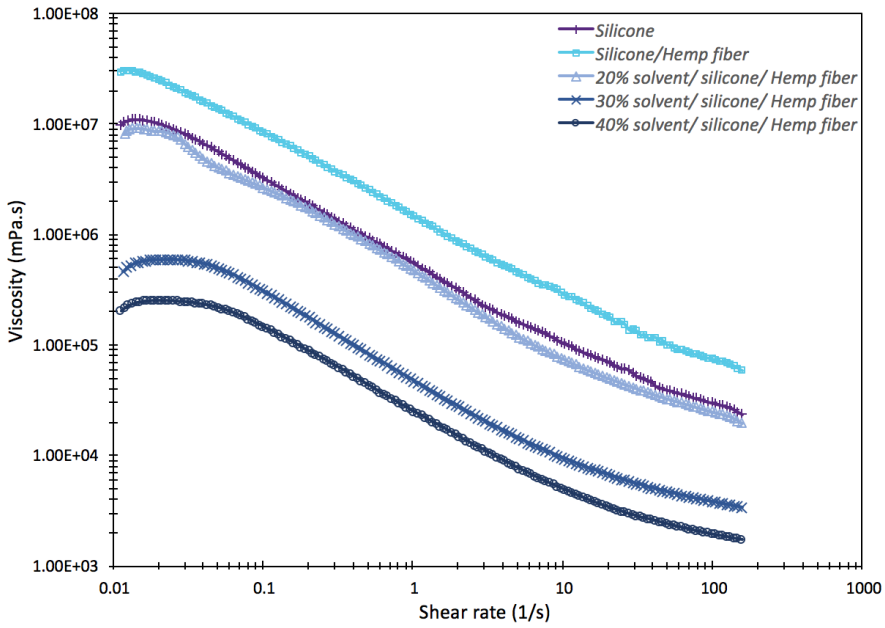

Figure 33: Shear-viscosity results for all experimental samples.

4.3.1 Rheological evaluation

Rheological studies were executed to measure viscosity, recovery behavior, and yield stress of silicone/hemp fiber composites containing different solvent concentration. These rheological tests describe the properties of the inks before, during and after being extruded in the printing process.

Shear thinning characterisation

Figure 33 demonstrates the shear viscosity profiles of all the samples which were measured by rheology measurements. All experimental samples displayed shear thinning behavior in which the viscosity decreases over increasing shear rate. The 30 (wt%) and 40 (wt%) solvent, demonstrate significantly lower viscosities compared to silicone. The composition containing 20 (wt%) solvent, aligned very closely in shear thinning characteristics to printable pure silicone. In other words, the shear thinning profile for the 20 (wt%) solvent is similar to pure silicone. Material slipping out between plates at higher shear rate led to difficulties in the shear-viscosity measurements and caused inconsistencies at higher shear rate. Therefore, high shear rates (more than $100s^{-1}$) were excluded from these experiments.

Recovery behaviour

Recovery testing was performed to analyze shape fidelity after 3D printing for all specimens. As the rheometer cannot measure the viscosity at true zero-shear, shear rate of $0.01s^{-1}$ was chosen to mimic at-rest condition during printing. To simulate the condition in the nozzle tip a shear force of $100s^{-1}$ was applied to the samples for 100s (calculation for shear rate inside nozzle was explained in experimental procedures chapter, section 3.4.2). Finally, to measure the recovery of the materials a low shear rate of $0.01s^{-1}$ was again applied. Figure 34 demonstrates the recovery results for

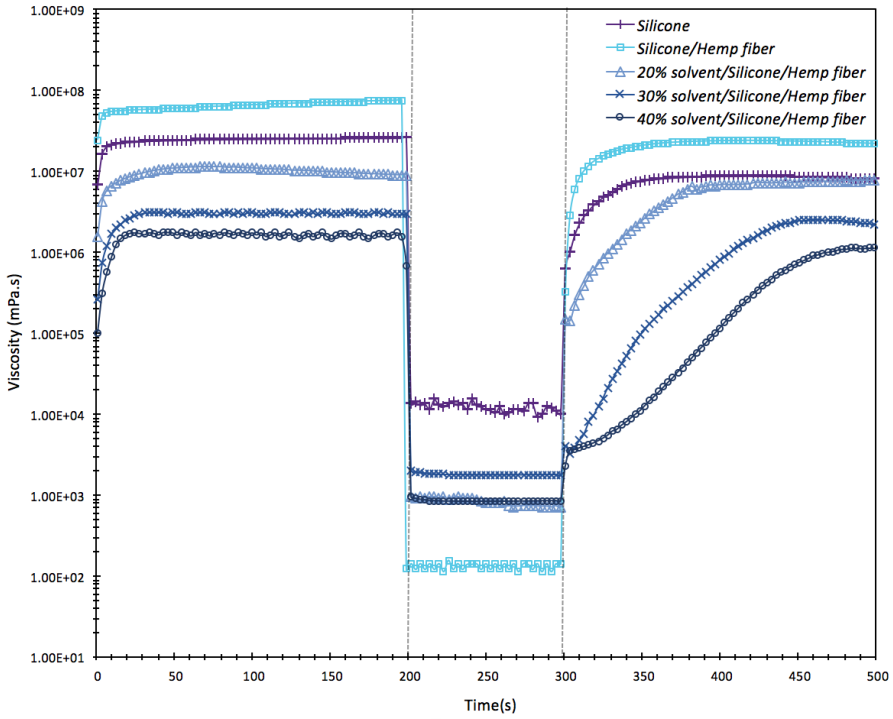

Figure 34: Recovery behavior of experimental samples to determine material behavior under a shear rate ($100s^{-1}$) to near-zero shear to simulate the environment experienced by the materials during extrusion printing.

different solvent concentrations. Here, the pure silicone show rapid recovery (50 s) after exposing under high shear rate. This behavior makes the material to quickly increase its viscosity after extruding and keep its shape after depositing. It can be observed that it takes 140 s for the sample containing 30 (wt%), and 40 (wt%) solvent to get steady in viscosity which causes difficulties in formation of continuous flow and shape fidelity. This is another evidence that samples with 30 and 40 (wt%) solvent

are showing unprintability characteristics. However, the composition containing 20 (wt%) solvent exhibits shorter recovery time to its initial viscosity in less than 75 s. Therefore, 20 (wt%) solvent concentration exhibits closer printability characteristics to pure silicone.

Yield stress measurements

Yield stress is an important parameter in determining printability. Shear stress ramp test was performed to measure the yield stress of the hemp fiber/silicone with different solvent composition. Figure 35 demonstrates the viscosity-shear stress curves which give information about yield stress. Yield stress was determined using the intersection of the plateau region in which the material is deformed elastically, and the region that the viscosity drops and the material starts to flow.

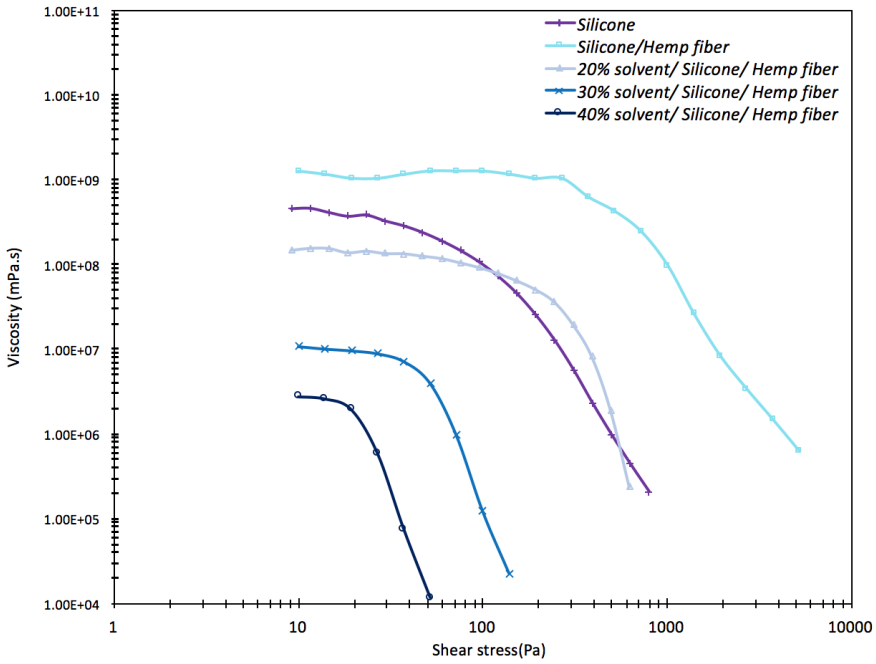

Figure 35: Shear stress ramp for all experimental samples.

Table 11 summarizes the results for different composition containing different solvent concentration. By comparison, the hemp fiber/ reinforced silicone sample without solvent displayed highest yield stress which justified material capability to keep its shape after printing. However, this composition exhibited high viscosity which makes it unprintable. The composition containing 20 (wt%) solvent also displayed higher yield stress compared with silicone. In other words, the composition containing 20 (wt%) solvent has higher ability to keep its shape after fabrication compared with silicone due to its high yield stress.

Table 11: Yield point of the different samples.

	Yield stress(Pa)
Silicone	85.40
Silicone/Hemp fiber	440.76
Silicone/Hemp fiber/20(wt%) solvent	152.64
Silicone/Hemp fiber/30(wt%) solvent	45.79
Silicone/Hemp fiber/40(wt%) solvent	21.82

4.3.2 Physical validation

To confirm rheological results, material flow was also monitored during manual extrusion. Figure 36 demonstrates the material flow for different samples with different composition. 10 (wt%) (Figure 36 (a)) displayed the curling effect which rendered it unprintable as it was cured so fast. 30 (wt%) (Figure 36 (c)) displayed partial fiber formation, however material flow was inconsistent and short. 40 (wt%) (Figure 36 (d)) demonstrated droplet formation and could not form consistent material flow. Therefore, both 30 and 40 (wt%) also exhibited unprintable behavior in line with rheological results. On the other hand, 20 (wt%) solvent (Figure 36 (b)) showed continuous and consistent material flow which are the required characteristics for 3D printability.

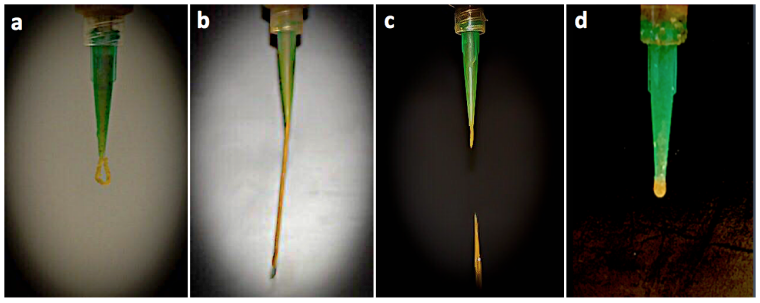

Figure 36: Effect of solvent concentration on material flow; a) 10 (%) solvent b) 20 (%) solvent c) 30 (%) solvent d) 40 (%) solvent.

In addition, hexagon honeycomb structures were 3D printed to determine shape fidelity characteristics of different compositions. Figure 37 shows 3D printed hexagon honeycomb structures with 40, 30, 20 (wt%) solvent concentrations over curing process. The images clearly show that structures containing 40 and 30 (wt%) solvent concentrations did not keep the hexagon shape over the curing process. On the other hand, the honeycomb structure containing 20 (wt%) solvent maintained the hexagon shape. These observations, are in agreement with rheological results.

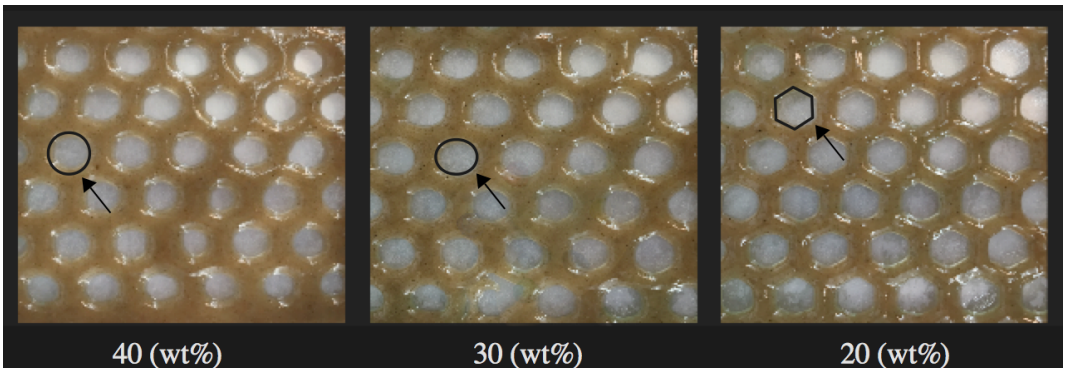

Figure 37: Effect of solvent concentration on 3D printing shape fidelity.

From rheological evaluation and physical validation, it is concluded that the composition containing 15 (wt%) hemp fiber and 20 (wt%) solvent had the capability to form continuous flow and maintain its shape which are required for 3D printing.

4.3.3 Rheological behavior of final printed composites

After determining 15 (wt%) hemp fiber/silicone containing 20 (wt%) solvent as the desirable composition time sweep test was performed to study dynamic mechanical behavior over curing time. Figure 38 illustrates an improvement in storage modulus over time for hemp fiber reinforced silicone composite compared with pure silicone. This enhancement is due to the higher restriction executed by the fibers on the matrix, which increased the stress transfer at the fiber interface.

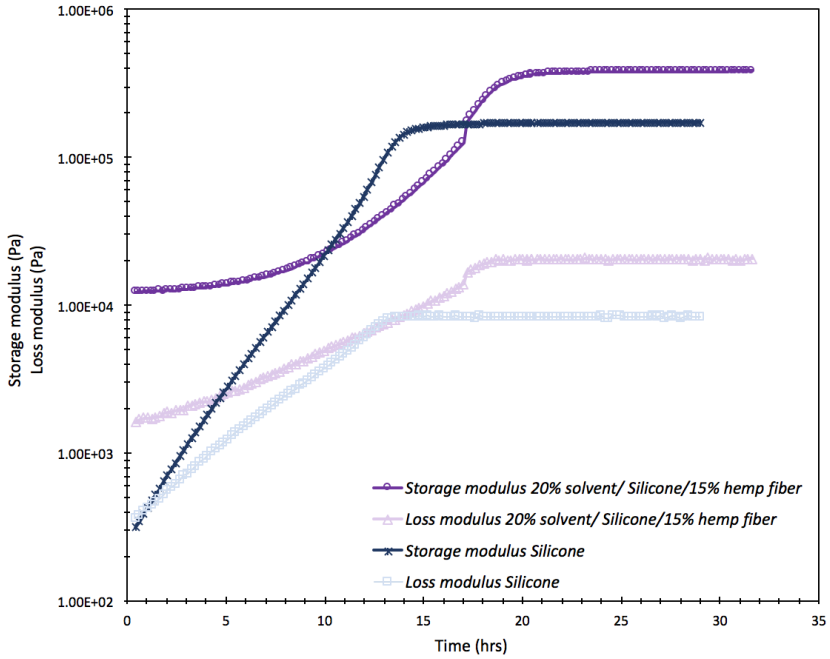

Figure 38: The effect of hemp fibers on shear storage modulus of silicone.

As expected the pure silicone behavior was dominated by loss modulus until the gel point which is the point where it converted from viscous fluid structure to elastic structure. The hemp fiber reinforced composites behavior was dominated by the storage modulus throughout the entire curing time. Due to the incorporation of filler, the composite demonstrates solid like behavior. This elastic characteristic of the material is confirming the material capability to maintain its shape until it's cured over time.

4.4 Effect of 3D printing on mechanical properties of hemp fiber reinforced silicone

In order to determine impact of 3D printing on mechanical properties, dog bone shape samples were 3D printed (parts printed at 0° angle). Figure 39 demonstrates the tensile strength and young's modulus of 3D printed hemp fiber reinforced silicone composites. It is evident that the printed samples have higher stiffness and tensile strength in comparison with non-printed samples. Indeed, 3D printed samples possess higher mechanical properties due to a densification of the paste as it's extruded through the nozzle.

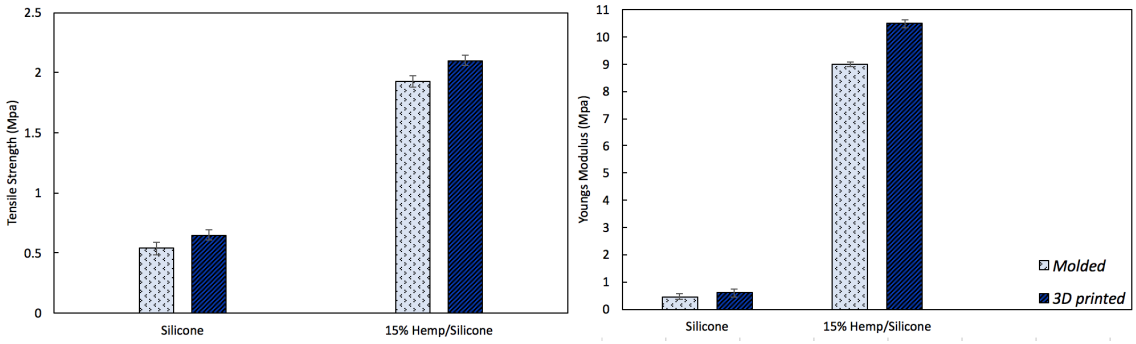

Figure 39: Mechanical properties of 3D printed products

Figure 40 shows the surface fractured of 3D printed and molded samples after tensile test. SEM images demonstrate the extent of void inclusion in molded samples. Indeed, there are large voids within the molded samples compared to 3D printed samples with the same composition.

It shows that the bubbles were removed as the material passed through the nozzle. Therefore, the 3D printed product has a denser structure leading to improved mechanical properties.

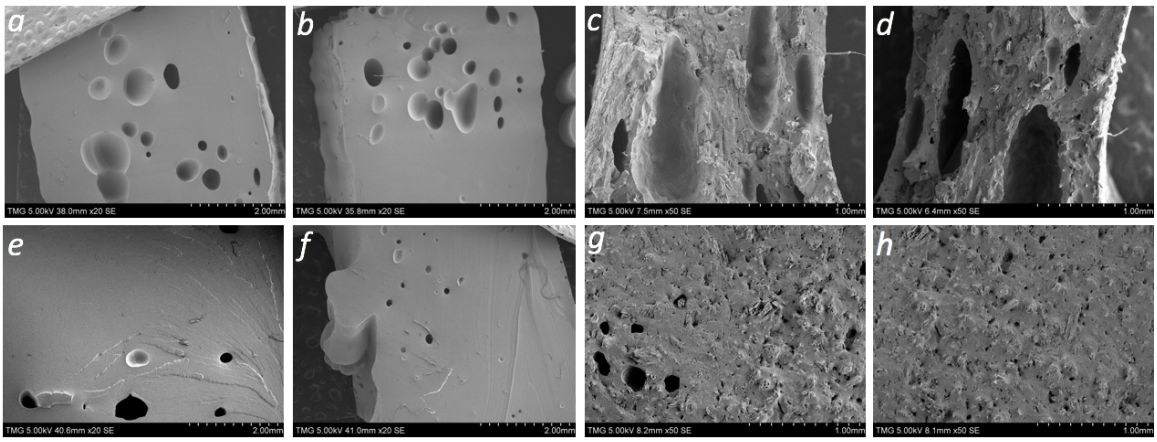

Figure 40: Cross-section of 3D printed and molded samples a,b)Cross-section of molded silicone c,d) Cross-section of 3D printed silicone e,f) Cross-section of molded hemp fiber reinforced silicone g,h) Cross-section of 3D printed hemp fiber reinforced silicone.

In addition, The enhanced mechanical properties could be explained by the fact that hemp fibers were aligned during 3D printing process. SEM images show the directional alignment of hemp fibers along printing direction. In contrast, for molded samples, there is no fiber alignment.

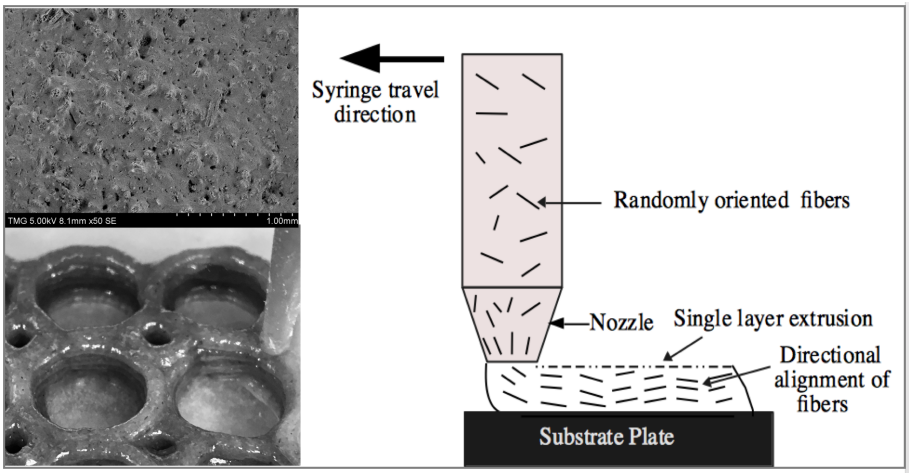

Figure 41: Effect of 3D-printing on fiber's orientation.

Direct ink writing (DIW) is an extrusion-based 3D printing in which fibers are distributed randomly before they reached to nozzle tip and aligned under the shear and extensional flow field that applied by nozzle during 3D printing. In fact, under the simple shear flow fibers tend to align in the shear direction (Figure 41). Figure 42 shows directional alignment of hemp fibres along the scanning/printing direction. This is leading to higher mechanical properties compare to those fabricated by mold

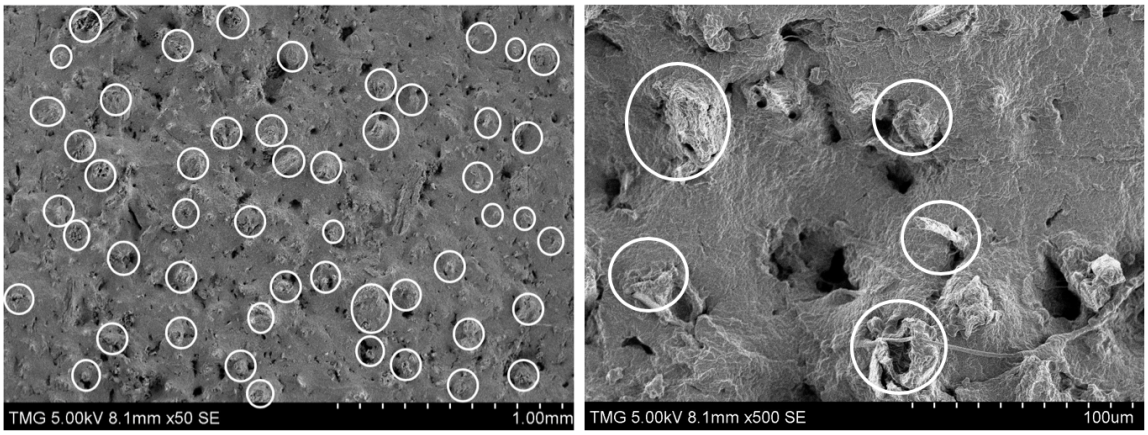

Figure 42: Hemp fibers were aligned during extrusion.

4.5 Applications

4.5.1 Soft robotics

Conventional molding methods to fabricate soft robots are difficult, time-consuming procedures, and highly dependent on manual handling. Therefore, in this study advanced manufacturing 3D printing technology was employed to fabricate a simple soft gripper based on silicone/hemp fiber and it was compared with its silicone counterparts (Figure 43).

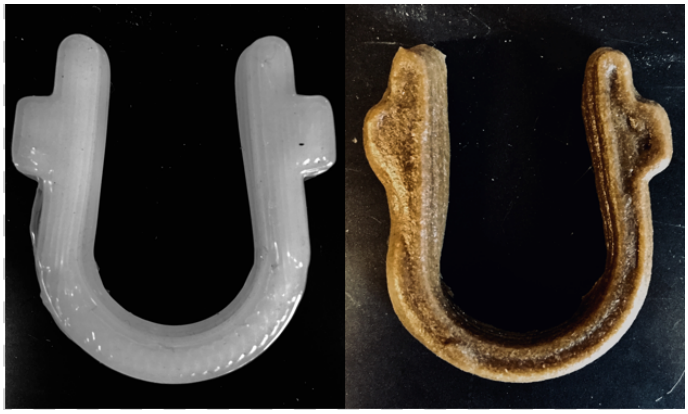

Figure 43: Simple gripper fabricated using DIW 3D printing method.

In order to make a comparison between the strength of the two grippers, a micro force sensor was used. To prevent unwanted movements the soft grippers were held on a flat plate. An adjustable angle clamp was used to provide the same situation for each soft gripper. In other words, the clamps were fixed during measurement and the grippers were inserted between them. Figure 44 shows that there is a significant difference in measured micro sensor voltage between the silicone gripper and silicone reinforced by hemp fiber gripper.

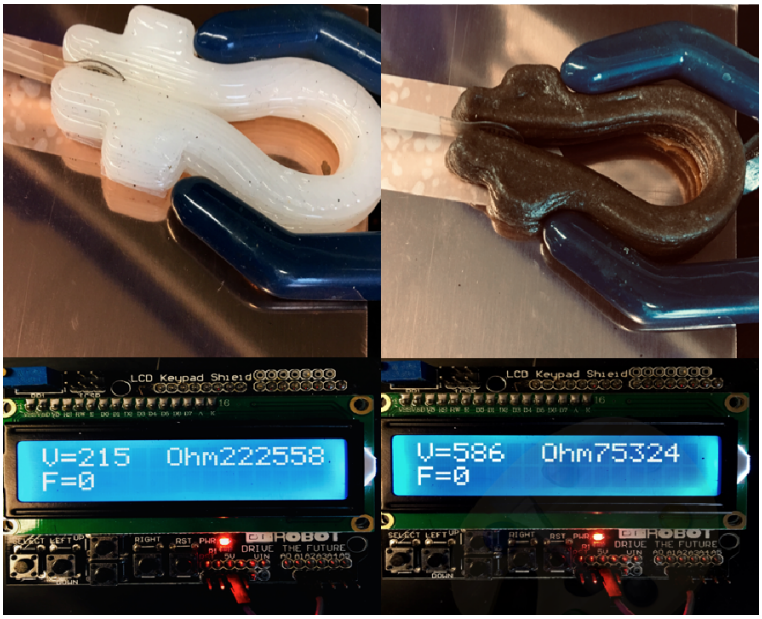

Figure 44: Using micro force sensor to find the differences between two grippers.

Figure 45 is used to convert the voltage into weight and it shows that the silicone/hemp fiber gripper is capable of lifting around 130 grams, however, the silicone gripper can lift around 30 grams. Therefore, incorporation of hemp fibers significantly affected silicone properties and made it stronger. The silicone/hemp base gripper can efficiently grip heavier objects, while its silicone counterpart cannot grasp objects with the weight above 30 grams.

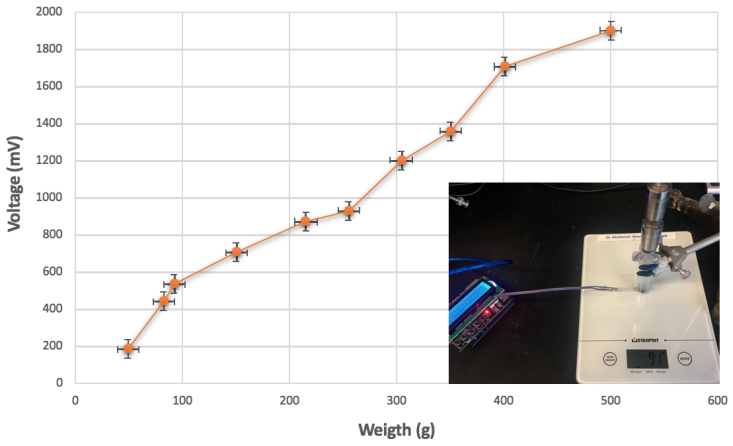

Figure 45: Voltage as a function of weight.

4.5.2 Biomedical engineering

Recently, elastomeric blends and composites have been utilized in a wide range of biomedical applications including vascular grafts, cardiac assist pumps, blood bags, and implants. These elastomeric composites provide advantages like biocompatibility and biodegradability, and acceptable mechanical properties [74]. Chandramohan et al. [75] developed biocomposites based on natural fibers and epoxy resins and investigated their desirability as a replacement of orthopedic alloys. It was revealed that the biocomposites based on sisal and roselle fibers are appropriate for being applied for both internal and external fixation on the human body. As cartilage tissue gets hurt during daily life especially in the elderly, many reviews have been done on the development and testing of composites scaffolds for the tissue engineering of articular cartilage. Pei et al. [76] worked on hydrogel scaffolds based on silk fibers. Their study demonstrated that the reinforced biocomposites have achieved optimal load bearing which is similar to cartilage tissue.

In this study, a silicon/hemp fiber honeycomb structure was fabricated using 3D printing (Figure 46), to show that it is possible to manufacture complex light-weight structures which have biomedical applications.

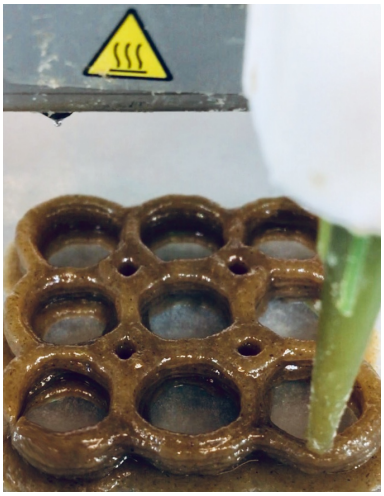

Figure 46: Fabrication of honeycomb structure with hemp fiber reinforced silicone composite.

Chapter 5

Conclusion and Future works

5.1 Conclusion

This study presented the design of a new printable material developed by incorporation of hemp fiber in silicone elastomers with enhanced mechanical properties. In other words, the idea of this work was to design new printable material with high functionalities. To enhance hemp fiber/silicone composites mechanical properties and to ensure its printability, it was required to determine suitable mixing composition. Therefore, mechanical tests and microscopic examinations were used to figure out the hemp fibers loading which provided desirable mechanical properties. Incorporation of 15 (wt%) fiber increased tensile strength and modulus of hemp fiber/silicone composites by 61% and 89% respectively, compared to silicone. Hence, 15% fiber loading was chosen as a suitable candidate.

One of the main drawbacks of natural fibers polymer composites is the poor compatibility between the fibers and matrix. Therefore, alkali and silane treatments were used to modify the surface of hemp fibers. Alkali and silane treatments improved tensile strength and modulus of hemp fiber/silicone composites by 27% and 54% respectively, compared to the composition containing untreated hemp fibers. Alkali treatment increased the surface roughness of the hemp fiber and exposed more reactive OH groups on the fiber surface to facilitate chemical bonding. On the other hand, silane coupling agent acts as a bridge between hemp fiber and silicon. Therefore, silane treatment increased the fiber-matrix interfacial bonding strength resulted in enhanced mechanical properties.

In this study, hemp fiber silicone composite was 3D printed using hemp fiber as the feedstock material and silicone as the binder. The challenge with 3D printing this material was the high viscosity which made them unprintable. Different solvent concentrations were added to the composition to determine the composition with printable behavior. Two-step printability assessment was performed to obtain printable material; rheological evaluation and physical validation. Rheological evaluations provided a clear understanding of the material behavior during the entire 3D printing process; in other words, during extrusion, material deposition and curing. While manual extrusion was performed to obtain information about flow formation at the tip of the nozzle during the extrusion. The results revealed that hemp fiber/silicone composition containing 20 (%wt) solvent exhibited 3D printable behavior. Based on rheological studies and physical validation, this composition was capable to form continuous

flow and keep its shape after deposition. Mechanical testing demonstrated that 3D printed products have improved mechanical properties compared to the molded samples. Improved mechanical properties were explained by densification of the paste as it was extruded through the nozzle, and fibers alignment made by the printing process.

Finally, by employing Direct ink writing 3D printing method, a simple gripper was fabricated based on silicone and compared to its silicone hemp fiber counterpart. The results demonstrated that the silicone hemp fiber gripper applied higher force than silicone gripper. Indeed, incorporation of fibers makes the gripper more strong and reliable.

5.2 Future work

In this study, an inexpensive silicone rubber with low mechanical properties was used, and it was justified that incorporation of hemp fibers increased tensile strength and young's modulus by 61% and 89% respectively. Hemp fibers from renewable resources have the capability to be used as a reinforcement material for another silicone matrix with high mechanical properties. For instance, two component silicone material has higher tensile strength compared with one component silicone. For instance, Ecoflex^{TM} 00-35 is a two components silicone with 5 minutes curing time. By using two components silicone, fibers could be dispersed homogeneously in matrix by increasing mixing time. Therefore, fibers could be dispersed in part A, and the crosslink agent will added to this composition during 3D printing. For fabricating this kind of materials there is advanced Discov3ry paste extruder providing the capability of co-extrusion of two different materials simultaneously with complete material mixing just before extrusion. This way one syringe can be filled by hemp fiber and crosslink agent, and the separate syringe would be dedicated to silicone. Therefore, two components could be mixed completely just before extrusion. This method will give us this opportunity to 3D print complicated and hollow structures, as the material would be cured right after injection.

In this research, effect of 3D printing on tensile strength and young's modulus was studied. Evaluate influence of 3D printing on other characteristics like durability and physical properties is recommended for future works.

In addition, polymers have great applications in sound and vibration damping for noise control in automobiles and airplanes. Many studies have been done on damping properties of magnetorheological elastomers [77, 78], but few studies have been done on damping characteristics of natural fibers reinforced elastomers [79]. Geethamma et al. [80] studied the dynamic mechanical behavior of short coir fiber reinforced natural rubber composites, and investigated the effect of fiber loading and interfacial bonding on damping properties. Dynamic behavior of fiber reinforced composite provides information about damping. It was demonstrated that increasing fiber loading increases heat dissipation in the designed composites [81], and improved damping properties. This study demonstrated (in Results and Discussion Chapter, Section Time Sweep) that incorporation of hemp fibers increased loss modulus in hemp fiber/ silicone composites. Therefore, this composition has the potential capability to be used in sound

and vibration damping for noise control.

Bibliography

[1] P. Song, Z. J. Peng, Y. L. Yue, H. Zhang, Z. Zhang, and Y. C. Fan. Mechanical properties of silicone composites reinforced with micron-and nano-sized magnetic particles. *Express Polymer Letters*, 7(6), 2013.

[2] A. K. Bledzki, V. E. Sperber, and O. Faruk. *Natural and wood fibre reinforcement in polymers*, volume 13. iSmithers Rapra Publishing, 2002.

[3] G. Momen and M. Farzaneh. Survey of micro/nano filler use to improve silicone rubber for outdoor insulators. *Rev. Adv. Mater. Sci*, 27(1):1–13, 2011.

[4] M. Thiruchitrambalam, A. Athijayamani, s. Sathiyamurthy, and A. Thaheer. A review on the natural fiber-reinforced polymer composites for the development of roselle fiber-reinforced polyester composite. *Journal of Natural Fibers*, 7(4):307–323, 2010.

[5] A. B. Asha, A. Benozir, A. Sharif, and M. D. Enamul Hoque. Interface interaction of jute fiber reinforced pla biocomposites for potential applications. In *Green Biocomposites*, pages 285–307. Springer, 2017.

[6] M. Brahmakumar, C. Pavithran, and R.M. Pillai. Coconut fibre reinforced polyethylene composites: effect of natural waxy surface layer of the fibre on fibre/matrix interfacial bonding and strength of composites. *Composites Science and Technology*, 65(3):563 – 569, 2005. JNC13-AMAC-Strasbourg.

[7] Karthikeyan and Rajasekaran. *Analysis of Natural Fiber Orientation in Polymer Composites Produced by Injection Molding Process*. PhD thesis, University of Toronto (Canada), 2017.

[8] R. Matsuzaki, M. Ueda, M. Namiki, T. K. Jeong, H. Asahara, K. Horiguchi, T. Nakamura, A. Todoroki, and Y. Hirano. Three-dimensional printing

of continuous-fiber composites by in-nozzle impregnation. *Scientific reports*, 6:23058, 2016.

[9] J. Rossiter, P. Walters, and B. Stoimenov. Printing 3d dielectric elastomer actuators for soft robotics. In *Electroactive Polymer Actuators and Devices (EAPAD) 2009*, volume 7287, page 72870H. International Society for Optics and Photonics, 2009.

[10] N. A. Nguyen, C. Bowland, and A. K. Naskar. A general method to improve 3d-printability and inter-layer adhesion in lignin-based composites. *Applied Materials Today*, 12:138 – 152, 2018.

[11] American Composites Manufacturers Association. What are composites, 2015. http://compositeslab.com/composites-101/what-are-composites/.

[12] UNSW Sydny. Fibre reinforced compposites, 2013. http://www.materials.unsw.edu.au/tutorials/online-tutorials/2-fibre-reinforced-compposites.

[13] Liliane Bokobza. Mechanical and electrical properties of elastomer nanocomposites based on different carbon nanomaterials. *C*, 3(2), 2017.

[14] Alice Pazat, Claire Barrès, Florence Bruno, Claude Janin, and Emmanuel Beyou. Preparation and properties of elastomer composites containing "graphene"-based fillers: A review. *Polymer Reviews*, 0(0):1–41, 2018.

[15] Z. Peng, C. Feng, Y. Luo, Y. Li, and L. X. Kong. Self-assembled natural rubber/multi-walled carbon nanotube composites using latex compounding techniques. *Carbon*, 48(15):4497 – 4503, 2010.

[16] Kapil Pandey. *Natural fibre composites for 3D Printing*. PhD thesis, Arcada, 2015.

[17] K. Okubo, T. Fujii, and Y. Yamamoto. Development of bamboo-based polymer composites and their mechanical properties. *Composites Part A: Applied Science and Manufacturing*, 35(3):377 – 383, 2004.

[18] Y. Zhang, Y. Li, H. Ma, and T. Yu. Tensile and interfacial properties of unidirectional flax/glass fiber reinforced hybrid composites. *Composites Science and Technology*, 88:172 – 177, 2013.

[19] N. Saba, M. T. Paridah, and M. Jawaid. Mechanical properties of kenaf fibre reinforced polymer composite: A review. *Construction and Building Materials*, 76:87 – 96, 2015.

[20] H. y. Cheung, M. P. Ho, K. T. Lau, F. Cardona, and D. Hui. Natural fibre-reinforced composites for bioengineering and environmental engineering applications. *Composites Part B: Engineering*, 40(7):655 – 663, 2009.

[21] P. Wambua, J. Ivens, and I. Verpoest. Natural fibres: can they replace glass in fibre reinforced plastics? *Composites Science and Technology*, 63(9):1259 – 1264, 2003. Eco-Composites.

[22] D. De, D. De, and B. Adhikari. Curing characteristics and mechanical properties of alkali-treated grass-fiber-filled natural rubber composites and effects of bonding agent. *Journal of applied polymer science*, 101(5):3151–3160, 2006.

[23] K. Hanhi, M. Poikelispää, and H. M. Tirilä. *ELASTOMERIC MATERIALS*. Tampere University, 2007.

[24] R. Malkapuram, V. Kumar, and Y. S. Negi. Recent development in natural fiber reinforced polypropylene composites. *Journal of Reinforced Plastics and Composites*, 28(10):1169–1189, 2009.

[25] J. Holbery and D. Houston. Natural-fiber-reinforced polymer composites in automotive applications. *JOM*, 58(11):80–86, 2006.

[26] M. S. Islam, K. L. Pickering, and N. J. Foreman. Influence of alkali treatment on the interfacial and physico-mechanical properties of industrial hemp fibre reinforced polylactic acid composites. *Composites Part A: Applied Science and Manufacturing*, 41(5):596 – 603, 2010.

[27] E. O. Cisneros-Lopez, M. E. Gonzalez-Lopez, A. A. Perez-Fonseca, R. Gonzalez-Nunez, D. Rodrigue, and J. O. RobledoOrtiz. Effect of fiber content and surface

treatment on the mechanical properties of natural fiber composites produced by rotomolding. *Composite Interfaces*, 24(1):35–53, 2017.

[28] F. F. Shuhimi, M. F. B Abdollah, M. A. Kalam, H. H. Masjuki, M. Ashafi'e, S. E. Mat Kamal, and H. Amiruddin. Effect of operating parameters and chemical treatment on the tribological performance of natural fiber composites: A review. *Particulate Science and Technology*, 35(5):512–524, 2017.

[29] S. Kalia, B. S. Kaith, and I. Kaur. Pretreatments of natural fibers and their application as reinforcing material in polymer composites—a review. *Polymer Engineering & Science*, 49(7):1253–1272, 2009.

[30] M. Jacob, S. Thomas, and K. T. Varughese. Mechanical properties of sisal/oil palm hybrid fiber reinforced natural rubber composites. *Composites Science and Technology*, 64(7):955–965, 2004.

[31] Y. Karaduman, L. Onal, and A. Rawal. Effect of stacking sequence on mechanical properties of hybrid flax/jute fibers reinforced thermoplastic composites. *Polymer Composites*, 36(12):2167–2173, 2015.

[32] S. Theresa, P. Selvum, K. Alastair, and N. Haibin. Hemp fiber reinforced polypropylene composites: The effects of material treatments. *Composites Part B: Engineering*, 114:15 – 22, 2017.

[33] D. Ray, B. K. Sarkar, A. K. Rana, and N. R. Bose. Effect of alkali treated jute fibres on composite properties. *Bulletin of Materials Science*, 24:129–135, 2001.

[34] Huang Gu. Tensile behaviours of the coir fibre and related composites after naoh treatment. *Materials & Design*, 30(9):3931–3934, 2009.

[35] D. Debasish, D. Debapriya, and A. Basudam. Curing characteristics and mechanical properties of alkali-treated grass-fiber-filled natural rubber composites and effects of bonding agent. *Journal of applied polymer science*, 101(5):3151–3160, 2006.

[36] D. Garcia, L. Quiles-Carrillo, N. Montanes, V. Fombuena, and R. Balart. Manufacturing and characterization of composite fibreboards with posidonia oceanica

wastes with an environmentally-friendly binder from epoxy resin. *Materials*, 11:35, 2017.

[37] M. S. Huda, L. T. Drzal, A. K. Mohanty, and M. Misra. Effect of fiber surface-treatments on the properties of laminated biocomposites from poly(lactic acid) (pla) and kenaf fibers. *Composites Science and Technology*, 68(2):424 – 432, 2008.

[38] M. Abdelmouleh, S. Boufi, M. N. Belgacem, and A. Dufresne. Short natural-fibre reinforced polyethylene and natural rubber composites: Effect of silane coupling agents and fibres loading. *Composites Science and Technology*, 67(7):1627 – 1639, 2007.

[39] E. T. N. Bisanda and M. P. Ansell. The effect of silane treatment on the mechanical and physical properties of sisal-epoxy composites. *Composites Science and Technology*, 41(2):165 – 178, 1991.

[40] B. Mosadegh, P. Polygerinos, C. Keplinger, S. Wennstedt, R. F. Shepherd, U. Gupta, J. Shim, and K. Bertoldi. Pneumatic networks for soft robotics that actuate rapidly. *Advanced functional materials*, 24(15):2163–2170, 2014.

[41] Fred R Sias. *Lost-wax casting: old, new, and inexpensive methods*. Woodsmere Press, 2005.

[42] A. D. Marchese, R. K. Katzschmann, and D. Rus. A recipe for soft fluidic elastomer robots. *Soft Robotics*, 2(1):7–25, 2015.

[43] O. D. Yirmibesoglu, J. Morrow, S. Walker, W. Gosrich, H. Kim, and U. Daalkhaijav. Direct 3d printing of silicone elastomer soft robots and their performance comparison with molded counterparts. In *2018 IEEE International Conference on Soft Robotics (RoboSoft)*, pages 295–302. IEEE, 2018.

[44] R. L. Truby and J. A. Lewis. Printing soft matter in three dimensions. *Nature*, 540(7633):371, 2016.

[45] X. Wang, M. Jiang, Z. Zhou, J. Gou, and D. Hui. 3d printing of polymer matrix composites: A review and prospective. *Composites Part B: Engineering*, 110:442 – 458, 2017.

[46] S. H. Huang, P. Liu, A. Mokasdar, and L. Hou. Additive manufacturing and its societal impact: a literature review. *The International Journal of Advanced Manufacturing Technology*, 67(5):1191–1203, Jul 2013.

[47] T. D. Ngo, A. Kashani, G. Imbalzano, K. Nguyen, and D. Hui. Additive manufacturing (3d printing): A review of materials, methods, applications and challenges. *Composites Part B: Engineering*, 143:172 – 196, 2018.

[48] M. C. Kuo, C. M. Tsai, J. C. Huang, and M. Chen. Peek composites reinforced by nano-sized sio2 and al2o3 particulates. *Materials Chemistry and Physics*, 90(1):185 – 195, 2005.

[49] S. P. Anil and C. Nachiket. Mechanical properties of tio2 and wc reinforced epoxy resin composites. *International Journal for Scientific Research*, 4, 2016.

[50] F. Castles, D. Isakov, A. Lui, Q. Lei, C. Dancer, Y. Wang, J. M. Janurudin, S. C. Speller, C. Grovenor, and P. S. Grant Patrick. Microwave dielectric characterisation of 3d-printed batio 3/abs polymer composites. *Scientific reports*, 6:22714, 2016.

[51] K. Pitt, O. Lopez-Botello, A. D. Lafferty, I. Todd, and K. Mumtaz. Investigation into the material properties of wooden composite structures with in-situ fibre reinforcement using additive manufacturing. *Composites Science and Technology*, 138:32 – 39, 2017.

[52] J. P. Lewicki, J. N. Rodriguez, C. Zhu, M. A. Worsley, and A. Wu. 3d-printing of meso-structurally ordered carbon fiber/polymer composites with unprecedented orthotropic physical properties. *Scientific reports*, 7:43401, 2017.

[53] Richard AL Jones. *Soft condensed matter*, volume 6. Oxford University Press, 2002.

[54] Hanna Watkin. Researchers develop stretchable elastomers for 3d printing, 2017. https://all3dp.com/researchers-develop-stretchable-elastomer-for-3d-printing/.

[55] Marion Willam. How 3d printing with silicones might change medical science, 2017. https://medium.com/healthcare-3d-printing-stories/how-3d-printing-with-silicones-might-change-medical-science-d54a398bce74.

[56] B. N. Peele, J. W. Thomas, Z. Huichan, and F. S. Robert. 3d printing antagonistic systems of artificial muscle using projection stereolithography. *Bioinspiration and Biomimetics*, 10(5):055003, 2015.

[57] S. Terryn, J. Brancart, D. Lefeber, G. Van Assche, and B. Vanderborght. Self-healing soft pneumatic robots. *Sci. Robot.*, 2(9), 2017.

[58] A. K. Bastola, V. T. Hoang, and L. Li. A novel hybrid magnetorheological elastomer developed by 3d printing. *Materials & Design*, 114:391–397, 2017.

[59] H. K. Yap, H. Y. Ng, and C. H. Yeow. High force soft printable pneumatics for soft robotic applications. *Soft Robotics*, 3(3):144–158, 2016.

[60] M. Huda, L. T. Drzal, A. K. Mohanty, and M. Misra. Effect of chemical modifications of the pineapple leaf fiber surfaces on the interfacial and mechanical properties of laminated biocomposites. *Composite Interfaces*, 15(2-3):169–191, 2008.

[61] F. Tavassoli, M. Razzaghi, and B. Mohebby. Hydrothermally treated wood as reinforcing filler for natural rubber bio-composites. *Journal of Polymer Research*, 25(1):3, 2018.

[62] Structur3d 3D printing. Ultimaker and the discov3ry paste extruder, 2018. https://www.structur3d.io/discov3ry-complete/.

[63] Ultimaker and the discov3ry paste extruder. `https://www.structur3d.io/discov3ry-complete/`.

[64] Mikolas Zuza. Everything about nozzles with a different diameter, 2018. https://www.prusaprinters.org/everything-about-nozzles-with-a-different-diameter/.

[65] R. Suntornnond, E. Y. Tan, J. An, and C. K. Chua. A mathematical model on the resolution of extrusion bioprinting for the development of new bioinks. *Materials*, 9(9):756, 2016.

[66] Q. H. Nguyen and N. D. Nguyen. Incompressible non-newtonian fluid flows. In *Continuum Mechanics-Progress in fundamentals and Engineering applications.* InTech, 2012.

[67] Malvern Panalitical. Using the power law model to quantify shear thinning behavior on a rotational rheometer, 2015. https://www.azom.com/article.aspx?ArticleID=11624.

[68] C. U. Maheswari, K. O. Reddy, E. Muzenda, M. Shukla, and A. V. Rajulu. Mechanical properties and chemical resistance of short tamarind fiber/unsaturated polyester composites: Influence of fiber modification and fiber content. *International Journal of Polymer Analysis and Characterization*, 18(7):520–533, 2013.

[69] J. A. Simao, V. B. Carmona, J. M. Marconcini, L. H. Mattoso, S. T. Barsberg, and A. R. Sanadi. Effect of fiber treatment condition and coupling agent on the mechanical and thermal properties in highly filled composites of sugarcane bagasse fiber/pp. *Materials Research*, 19(4):746–751, 2016.

[70] N. Lu, S. Oza, and I. Ferguson. Effect of alkali and silane treatment on the thermal stability of hemp fibers as reinforcement in composite structures. In *Advanced Materials Research*, volume 415, pages 666–670. Trans Tech Publ, 2012.

[71] K. O. Reddy, C. U. Maheswari, K. R. Reddy, M. Shukla, E. Muzenda, and A. V. Rajulu. Effect of chemical treatment and fiber loading on mechanical properties of borassus (toddy palm) fiber/epoxy composites. *International Journal of Polymer Analysis and Characterization*, 20(7):612–626, 2015.

[72] M. Sabri, F. Hafiz, K. Shahril, and A. Rohana. Effects of silane coupling agent on mechanical properties and swelling behaviour of coconut fiber filled polypropylene composite. In *Advanced Materials Research*, volume 626, pages 657–661, 2013.

[73] M. Abdelmouleh, S. Boufi, M. Belgacem, and A. Dufresne. Short natural-fibre reinforced polyethylene and natural rubber composites: effect of silane coupling agents and fibres loading. *Composites science and technology*, 67(7-8):1627–1639, 2007.

[74] V. Kanyanta, A. Ivankovic, and N. Murphy. Bio-medical applications of elastomeric blends, composites. In *Advances in Elastomers II*, pages 227–252. Springer, 2013.

[75] D. Chandramohan and K. Marimuthu. Applications of natural fiber composites for replacement of orthopaedic alloys. In *Nanoscience, Engineering and Technology (ICONSET), 2011 International Conference on*, pages 137–145. IEEE, 2011.

[76] B. Pei, W. Wang, Y. Fan, X. Wang, F. Watari, and X. Li. Fiber-reinforced scaffolds in soft tissue engineering. *Regenerative biomaterials*, 4(4):257–268, 2017.

[77] G. V. Stepanov, D. Y. Borin, A. V. Bakhtiiarov, and P. A. Storozhenko. Magnetic properties of hybrid elastomers with magnetically hard fillers: rotation of particles. *Smart Materials and Structures*, 26(3):035060, 2017.

[78] M. Cvek, M. Mrlik, M. Ilčíková, J. Mosnáček, L. Münster, and V. Pavlinek. Synthesis of silicone elastomers containing silyl-based polymer-grafted carbonyl iron particles: An efficient way to improve magnetorheological, damping, and sensing performances. *Macromolecules*, 50(5):2189–2200, 2017.

[79] E. Jayamani, M. Bakri, and B. Khusairy. Lignocellulosic fibres reinforced polymer composites for acoustical applications. In *Lignocellulosic Composite Materials*, pages 415–444. Springer, 2018.

[80] V. G. Geethamma, G. Kalaprasad, and Sabu Thomas. Dynamic mechanical behavior of short coir fiber reinforced natural rubber composites. *Composites Part A: Applied Science and Manufacturing*, 36(11):1499 – 1506, 2005.

[81] R. Chandra, S. P. Singh, and K. Gupta. Damping studies in fiber-reinforced composites a review. *Composite Structures*, 46(1):41 – 51, 1999.